OCTOBER, 1950

RADIO & TELEVISION NEWS

RADIO-ELECTRONIC Engineering

TELEVISION

•

RADAR

•

ELECTRONICS

•

RESEARCH

•

COMMUNICATIONS

•

MAINTENANCE

RADIO & TELEVISION NEWS

RADIO-ELECTRONIC Engineering

Trade Mark Registered U. S. Patent Office No. 432907

ELECTRONICS • COMMUNICATIONS • TELEVISION • RESEARCH • MAINTENANCE

OCTOBER, 1950

WORK-COILS FOR H.F. HEATING .... R. A. Whiteman 3A

AN AMPLIFIER FOR MAGNETIC OSCILLOGRAPHS .... C. J. Tirk 7A

THE MONOFORMER .... Allen C. Munster 8A

ELECTRONIC FLUORESCENCE DETECTOR-COMPARATOR . . Charles Weeks 10A

RADIO NAVIGATION EQUIPMENT — PART 2 .... John P. Griffin 11A

MICROWAVE ANTENNAS .... J. Racker 15A

OFF-RESONANCE RESPONSE-LARGE DEVIATION .... Chester W. Young 32A

DEPARTMENTS

PERSONALS 22A

NEWS BRIEFS 24A

NEW PRODUCTS 26A

TECHNICAL BOOKS 29A

RADIO-ELECTRONIC ENGINEERING is published each month as a special edition in a limited number of copies of RADIO & TELEVISION NEWS, by the Ziff-Davis Publishing Company, 185 N. Wabash Avenue, Chicago 1, Illinois.

VOLUME 15, NUMBER 4, Copyright, 1950, Ziff-Davis Publishing Company

COVER PHOTO — Courtesy of Westinghouse Electric Corp.

A dichroic mirror, which will reflect only a certain color of light, being prepared at the Westinghouse Electric Corp. laboratories. While in a vacuum, special metal compounds are evaporated and condense on the glass. The thickness and number of layers deposited determine the color which is reflected.

ZIFF-DAVIS PUBLISHING COMPANY

WORK-COILS for H.F. HEATING

Fig. 1. Split type work-coil in load-

ied
ils.

upon the geometrical configuration of the work as well as the work-coil conductors. A detailed discussion of the advantages and disadvantages of different work-coil configurations will be included in this article.

There are two methods of approach to the study of the performance of a coil as a work-coil in induction heating. One is the electric-circuit concept as applied to the coil. This concept includes the lump electrical parameters as resistance and reactance and enables performance measurements to be made with the aid of a Q-meter. The other method, which is more academic in nature, considers the magnetic field in the vicinity of the work-coil as well

schematic representation as shown in Fig. 2.

The work-coil, as illustrated in Fig. 2, has an inductance L_c, a resistance R_c, and is supplied by a voltage E_c generated directly by a vacuum-tube

Fig. 2. Equivalent circuit of work-coil and conductive load showing work-coil current and work current electrically separated but magnetically coupled.

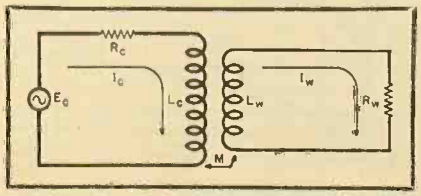

ndary of a current
ece of metal or the
nay be represented
g 2 by a resistance
an inductance L_w.
ance between the
coil is indicated by
tions for the work-
re:

$\omega MI_w = E_c$. (1)

$_w) I_w = 0$ . . (2)

in cycles per second and the inductances are in henrys. To obtain the input impedance to the loaded work-coil, these two equations are solved for the ratio of E_c to I_c or E_c/I_c. This ratio expressed algebraically is:

$$Z_c = R_c + \frac{(\omega M)^2 R_w}{R_w^2 + (\omega L_w)^2} + j\omega \left[L_c - \frac{(\omega M)^2 L_w}{R_w^2 + (\omega L_w)^2} \right] \quad . \quad . \quad (3)$$

This equation shows that the effective input resistance to the loaded work-coil is increased by the presence of the metallic load while the effective inductance has decreased.

For convenience of test measurement,

RADIO & TELEVISION NEWS

RADIO-ELECTRONIC Engineering

Trade Mark Registered U. S. Patent Office No. 432907

ELECTRONICS • COMMUNICATIONS • TELEVISION • RESEARCH • MAINTENANCE

OCTOBER, 1950

WORK-COILS FOR H.F. HEATING .... R. A. Whiteman 3A

AN AMPLIFIER FOR MAGNETIC OSCILLOGRAPHS .... C. J. Tirk 7A

THE MONOFORMER .... Allen C. Munste

ELECTRONIC FLUORESCENCE DETECTOR-COM

RADIO NAVIGAT

FIRST CLASS
Permit No. 3365
Sec. 34.9, P. L. & R.
CHICAGO, ILLINOIS

BUSINESS REPLY CARD
No Postage Necessary if Mailed in U. S. A.

2c Postage will be Paid by

Radio-Electronic Engineering
EDITION OF RADIO & TELEVISION NEWS
185 NORTH WABASH AVENUE
CHICAGO 1, ILLINOIS

of RADIO
Davis Publishing Company,
Chicago 1, Illinois.

OLUME 15, NUMBER 4, Copyright, 1950, Ziff-Davis Publishing Company

COVER PHOTO — Courtesy of Westinghouse Electric Corp.

A dichroic mirror, which will reflect only a certain color of light, being prepared at the Westinghouse Electric Corp. laboratories. While in a vacuum, special metal compounds are evaporated and condense on the glass. The thickness and number of layers deposited determine the color which is reflected.

WORK-COILS for H.F. HEATING

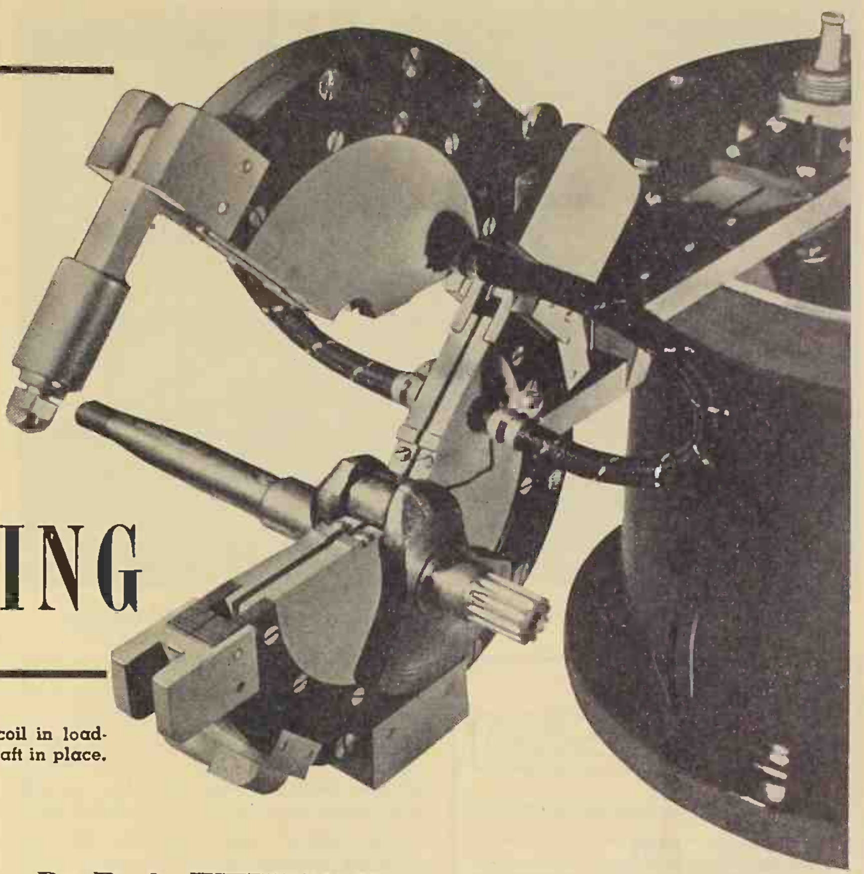

Fig. 1. Split type work-coil in loading position with crankshaft in place.

By R. A. WHITEMAN
Consulting Engineer, Chicago

Theoretical analysis and practical experimentation are combined to obtain the optimum design for induction heating work-coils.

THE application of induction heating to surface hardening, brazing, melting and annealing of metals requires suitably-designed work-coils in order to concentrate the heating effect to specific regions of the materials. To heat a metallic object by the induction method, it is placed in the vicinity of the work-coil and strong electric currents are induced in the object, thereby generating heat without contact. The distribution of the induced currents, and likewise the heat generated, depend upon the geometrical configuration of the work as well as the work-coil conductors. A detailed discussion of the advantages and disadvantages of different work-coil configurations will be included in this article.

There are two methods of approach to the study of the performance of a coil as a work-coil in induction heating. One is the electric-circuit concept as applied to the coil. This concept includes the lump electrical parameters as resistance and reactance and enables performance measurements to be made with the aid of a *Q*-meter. The other method, which is more academic in nature, considers the magnetic field in the vicinity of the work-coil as well as the power equations applied to the metallic load. This method provides a means of visualizing and computing the effects of changing the work-coil shape on the magnetic field as well as the coupling efficiency with the load. These two methods will be studied and their respective advantages applied to a number of applications.

The electric-circuit concept as applied to the study of the performance of a work-coil and conductive load is best understood by considering the schematic representation as shown in Fig. 2.

The work-coil, as illustrated in Fig. 2, has an inductance L_c, a resistance R_c, and is supplied by a voltage E_c generated directly by a vacuum-tube oscillator or the secondary of a current transformer. The piece of metal or the work to be heated may be represented electrically as in Fig 2 by a resistance R_w in series with an inductance L_w. The mutual inductance between the work and the work-coil is indicated by M. The circuit equations for the work-coil and the work are:

$$(R_c + j\omega L_c)\, I_c + j\omega M I_w = E_c \quad . \quad (1)$$

$$j\omega M I_c + (R_w + j\omega L_w)\, I_w = 0 \quad . \quad . \quad (2)$$

f is the frequency in cycles per second and the inductances are in henrys. To obtain the input impedance to the loaded work-coil, these two equations are solved for the ratio of E_c to I_c or E_c/I_c. This ratio expressed algebraically is:

$$Z_c = R_c + \frac{(\omega M)^2 R_w}{R_w^2 + (\omega L_w)^2} + j\omega \left[L_c - \frac{(\omega M)^2 L_w}{R_w^2 + (\omega L_w)^2} \right] \quad . \quad . \quad (3)$$

This equation shows that the effective input resistance to the loaded work-coil is increased by the presence of the metallic load while the effective inductance has decreased.

For convenience of test measurement,

Fig. 2. Equivalent circuit of work-coil and conductive load showing work-coil current and work current electrically separated but magnetically coupled.

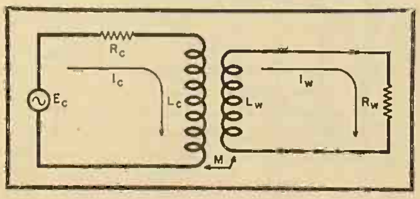

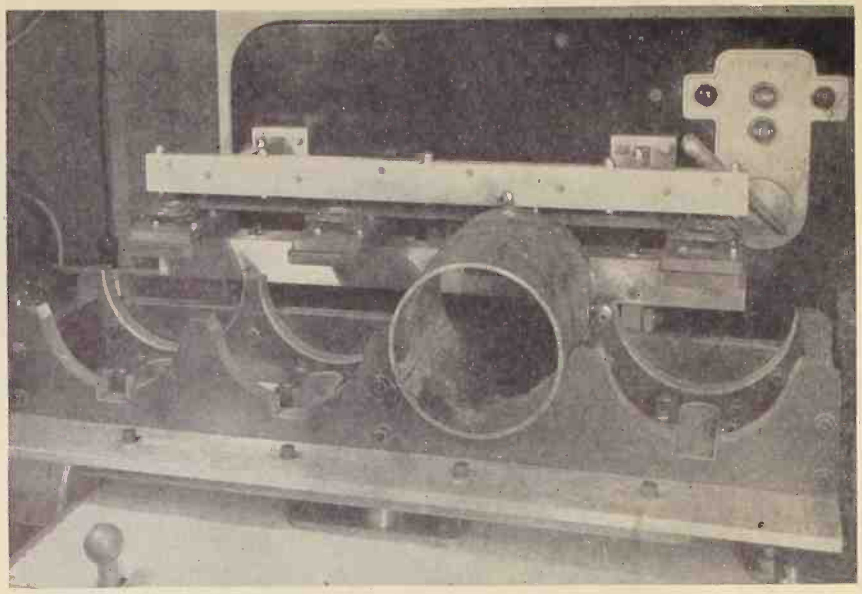

Fig. 3. Spiral-type work-coils for brazing suction fittings into compressor housings.

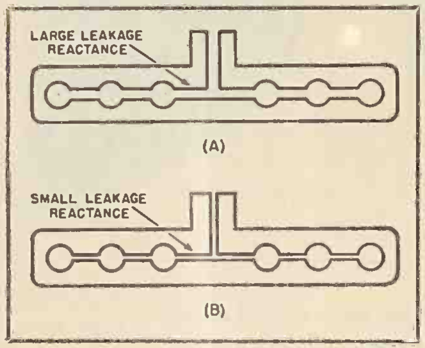

Fig. 4. (A) Poor arrangement of six work-coils in series. Leakage reactance is high, yielding low coupling efficiency. (B) Better arrangement with low leakage reactance and high coupling efficiency.

let $\omega L_w/R_w$ be the Q of the work or Q_w. Then the increase in the effective resistance due to the metallic load is:

$$\triangle R_c = \left(\frac{M}{L_w}\right)^2 R_w \frac{Q_w^2}{Q_w^2+1} \quad . \quad . \quad (4)$$

which will provide a method of evaluating the efficiency of the work-coil and work. The efficiency of the circuit illustrated in Fig. 2 is defined as the ratio of the power transferred to the load to the total power supplied to the terminals of the circuit. This ratio is:

$$\eta = \frac{\triangle R_c}{R_c + \triangle R_c} \quad . \quad . \quad . \quad . \quad . \quad . \quad . \quad (5)$$

and by substituting Eqt. (4) in (5) and assuming that Q_w is at least equal to or greater than 4, the efficiency formula reduces to:

$$\eta = \frac{\left(\frac{M}{L_w}\right)^2 \frac{R_w}{R_c}}{1 + \left(\frac{M}{L_w}\right)^2 \frac{R_w}{R_c}} \quad . \quad . \quad . \quad . \quad (6)$$

In order to facilitate the study of the general shape of the curve expressed by Eqt. (6), let the fundamental parameter K be equal to $(M/L_w)^2$ (R_w/R_c), and then the efficiency equation becomes:

$$\eta = \frac{K}{1+K} \quad . \quad . \quad . \quad . \quad . \quad . \quad . \quad . \quad (7)$$

This equation is plotted as a curve in Fig. 5 with the efficiency η plotted along the ordinate and K along the abscissa.

To illustrate the functional relations of the above circuit equations in a quantitative manner, consider the measurements and calculations made on a typical multi-turn work-coil closely coupled to a magnetic steel load. With the aid of a Q-meter operating at a frequency of one-half megacycle, the inductive reactance of the loaded coil was found to be 1.4 ohms and the corresponding effective resistance was .89 ohms. At one megacycle, the inductive reactance was measured as 2.85 ohms and the effective resistance was 1.18 ohms. A graph of these and other measurements together with the calculated work-coil efficiency is shown in Fig. 6. This example illustrates the application of the electric-circuit concept to the study of the performance of a typical work-coil.

A tremendous amount of design and experimental time applied to adjusting a work-coil can be saved by first evaluating the desired Q for the oscillator tank-circuit and then measuring the loaded tank-inductance with a Q-meter. This may be done with a reasonable degree of accuracy by using the formula:

$$Q = \omega\, CR_L \quad . \quad . \quad . \quad . \quad . \quad . \quad . \quad . \quad (8)$$

where R_L is the load impedance of the tank circuit and C is the tank capacitance. By disconnecting the inductance of the tank circuit from the tank capacitance, the tank inductance with work-coil and load are ready for Q-meter measurements. If the measured Q is greater than the computed value, the load impedance of the loaded work-coil is too high for the particular high-frequency voltage available and the power converted to heat in the load will be less than required. Likewise, if the measured Q is less than the computed value, the impedance of the work-coil will be too low and considerably more power will be absorbed by the load than desired. The numerical value of the Q of this circuit may be decreased or increased as desired, by either of several adjustments or by taking advantage of all of them. These adjustments consist of increasing or decreasing the coefficient of coupling with the load, changing the number of turns of the work-coil and as a last resort changing the capacitance of the tank circuit which will also change the frequency of operation. The effects of these adjustments are quickly and easily observed with the aid of a Q-meter, thereby simplifying the procedure of work-coil design.

One very important method of increasing the coefficient of coupling between a work-coil and the work is that of reducing the leakage inductive reactance. This will, of course, reduce the Q of the tank circuit as well as the reactive circulating current. A reduction of the leakage inductive reactance can be accomplished by decreasing unnecessary areas enclosed by the leads

Fig. 5. Variation of coupling efficiency with parameter K showing a high efficiency for K greater than four.

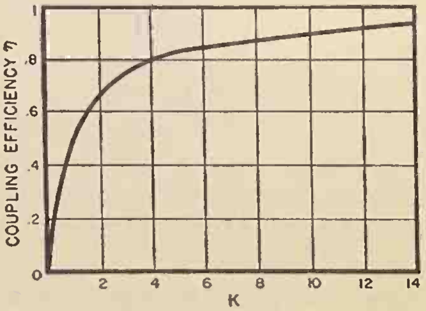

Fig. 6. Efficiency curve with reactance and resistance vs. frequency for a work-coil loaded with magnetic steel.

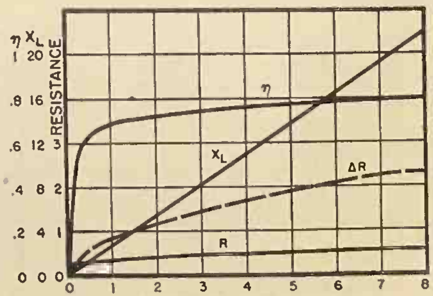

and other conductors of the work-coil. An example of a poorly arranged coil consisting of a group of 6 work-coils in series is shown in Fig. 4A. A much better arrangement of the conductors with less enclosed area is shown in Fig. 4B and as a result of this geometry, there is less leakage inductive reactance. An application of this type of series connection is shown in Fig. 8 and illustrates very well how the leakage-inductive reactance can be reduced to a very small value.

Another important factor that must be kept in mind when attempting to increase the coefficient of coupling is the cross-sectional shape of the work-coil conductor. If the cross-section of the conductor is circular and the coupling coefficient is not sufficient, it is possible to increase the coefficient by a few per-cent by using a conductor with an elliptical cross-section. The major axis of the ellipse should be perpendicular to the work surface. In fact the use of conductors with an elliptical cross-section will produce such a highly concentrated magnetic field that the temperature pattern will be extremely non-uniform.

Of all the various shapes and types of work-coils used for induction heating, the conduction material used in many applications is generally 3/16" or ¼" diameter copper tubing. The cooling of tubing type work-coils may be accomplished by passing water through the coil. It is interesting to note that this type of work-coil may be used as an internal or external coil for heating purposes. An arrangement of a typical coil for internal work is shown in Fig. 7A while a coil used for external work is shown in Fig. 7B.

There are applications of induction heating where a tubular work-coil can not be used because of the geometrical shape of the work. Any work to be heat treated that cannot pass through a tubular work-coil can be enclosed by a two-piece or split-type work-coil. This particular application is well illustrated by the split-type coil shown in the photograph of Fig. 1.

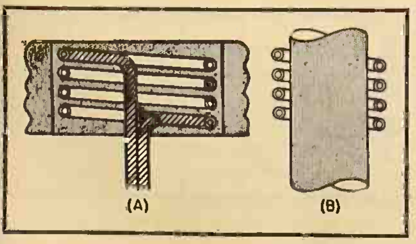

Fig. 7. (A) Constructional layout for an internal work-coil showing how to arrange coil leads close together. (B) Arrangement for external work-coil showing a constant pitch helix.

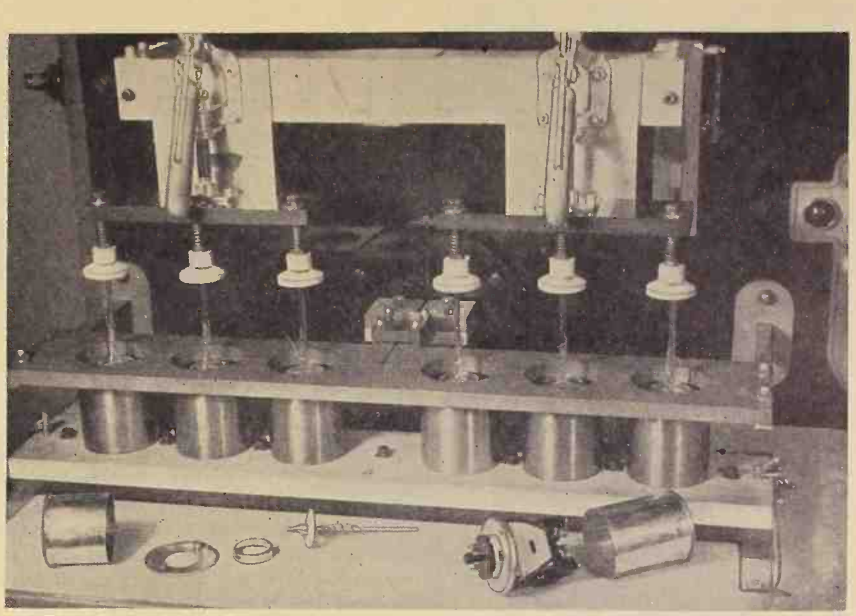

Fig. 8. Arrangement of six work-coils in series with small leakage reactance.

In this analysis of work-coils thus far, no consideration of the depth of penetration of the induced currents into the work has been made. It is important to note that the induced-current density is dependent upon the radius of curvature of the heated surface and that on a convex surface the depth of penetration will be greater and on a concave one less than $(C/2\pi)\sqrt{\rho/\mu f}$. This means that the induced-current density will be less at the tooth points than in the tooth spaces of a cam as well as a gear. Since the heat generated is proportional to the square of the induced-current density, less heat will be developed at the convex than at the concave surfaces.

This non-uniform distribution of the heat developed may be compensated somewhat by increasing the frequency of operation. The net effect is to decrease the depth of penetration and depend upon heat conduction to equalize the temperatures. If the shape of the work is such that the concave surface is adjacent to a large mass of metal, the heat developed will be conducted rapidly away from the concave surface and also compensate for the higher heat intensity.

Furthermore, it is important to emphasize that when the depth of penetration of the induced currents in the work is much less than the over-all dimensions, then neither the resistivity ρ nor the permeability μ of the materials will affect the distribution of peripheral density of the induced currents. The distribution of the magnetic field strength under such conditions will be about the same for both steel and copper. The values of ρ and μ will affect only the depth of penetration and the actual amount of heat generated by induced currents in the surface layers of the metal.

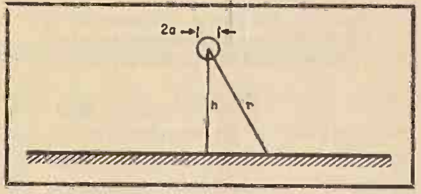

Fig. 9. A current-carrying conductor above a sheet of conducting material.

Although it is customary to think of a tubular coil in the shape of a helix to have a constant pitch, it has been advisable and in some applications necessary to use a variable pitch coil. It is erroneously believed by some, that the depth of penetration depends upon the pitch of the work-coil, but the depth of penetration is actually given by the formula $(C/2\pi)\sqrt{\rho/\mu f}$. The magnetic field intensity does depend upon the pitch of the helix and consequently determines the power developed in the surface layer extending to the depth of penetration. As the pitch of the coil is decreased and the magnetic field intensity increased, the power will in-

Fig. 10. Current-carrying circuit C, illustrating Ampere's law.

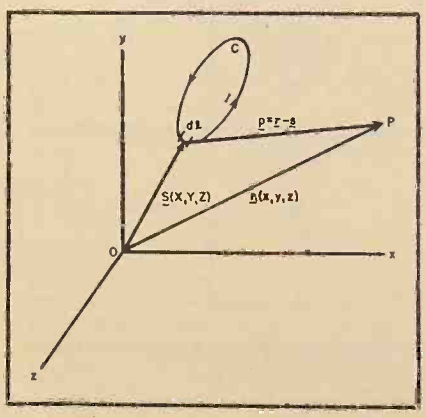

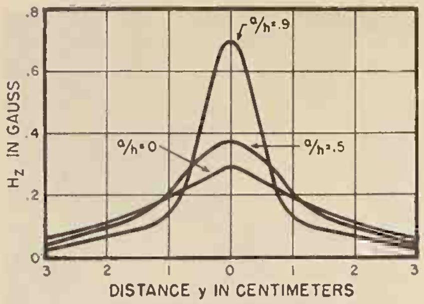

Fig. 11. Magnetic field intensity in a conducting sheet due to a single current carrying conductor.

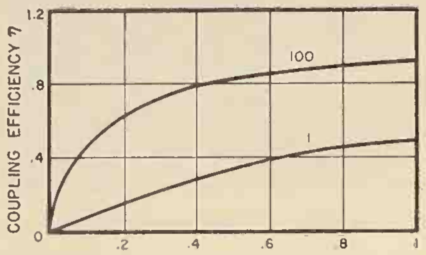

Fig. 13. Coupling efficiency of a conductor over a conducting sheet of material for two values of $\mu_w \sigma_c / \sigma_w$

crease and the temperature will rise more rapidly to its required point, but the depth of penetration remains the same. Of course, if the power is developed for the same period of time, the heat energy will extend beyond the depth of penetration due only to conduction.

It is because of heat conduction that the depth of heat treatment is greater on a surface closer to the turns of a work-coil. An off-center piece of metal within a work-coil will have more power developed per square inch of surface but the depth of penetration is the same. A practical approach to compensate for this variation in manufacturing processes is to rotate the load slowly at approximately 60 r.p.m. The motion of the work will distribute the higher and lower intensities of power over the entire heated area periodically so that the net result is a fairly uniform heat treatment instead of a non-uniform heating effect.

Fig. 14. (A) Two, and (B) three current-carrying conductors above a sheet of conducting material.

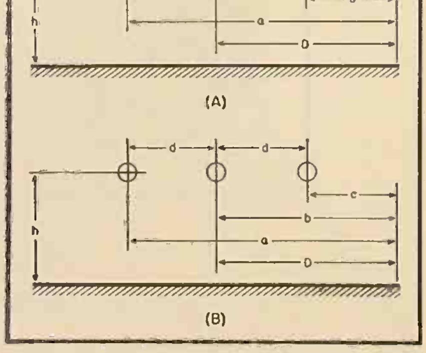

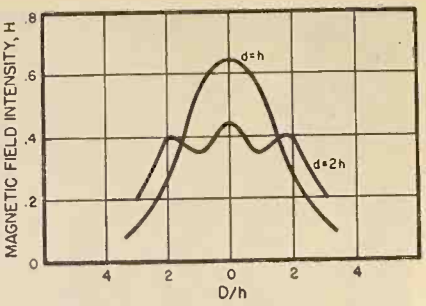

Fig. 12. Magnetic field intensity in a conducting sheet of material under a three-conductor work-coil.

The problem of obtaining a satisfactory efficiency and performance of a work-coil is not too difficult to solve by the trial and error method when the coil is a simple helix; however, for a great many applications a special coil shape is necessary and an understanding of the performance of a number of basic shapes is of great value.

To make this study of basic coil shapes as systematic as possible, it is advisable to introduce the second method of analyzing the efficiency and performance of work-coils. Since this method requires calculations which are different in detail for different coil shapes, a general method of calculating the coupling efficiency of an electromagnetic configuration will be presented. This general method is based upon a formula known as Ampere's law and is expressed algebraically as:

$$H = \int \frac{I \, dl \times \rho}{\sigma \quad \rho^3} \quad . \quad . \quad . \quad . \quad . \quad . \quad (9)$$

where these quantities are shown in Fig. 10 and represent the magnetic intensity vector H at a point P due to the electric circuit C. Point P is a distance ρ from the differential circuit element dl which in turn is carrying an electric current I. The integration is to extend over the entire electric circuit C. It is also necessary to note that the product indicated in Eqt. (9) is the Gibbs' vector product. Since the current density J is numerically equal to the magnetic field intensity vector H, Eqt. (9) may be substituted for J in the following equation which expresses the power developed in the work load. This equation is:

$$P_w = \frac{1}{\sigma_w S_w} \int_{-\infty}^{+\infty} J_w{}^2 \, dx \quad . \quad . \quad (10)$$

where σ_w is the conductivity of the work load and S_w the depth of penetration. Likewise, the power dissipated in the work coil is

$$P_c = \frac{1}{\sigma_c S_c} \int_{-\infty}^{+\infty} J_c{}^2 \, dx \quad . \quad . \quad . \quad (11)$$

where the corresponding quantities are for the work-coil instead of the work load. Of course, the evaluation of the integrals (10) and (11) is not accomplished in a simple manner unless the electromagnetic configuration is fairly simple. The evaluation of (10) and (11) will be given for a few basic arrangements so that the coupling efficiency η, already expressed in Eqt. (7), can be computed with the aid of:

$$\eta = \frac{P_w}{P_w + P_c} \quad . \quad . \quad . \quad . \quad . \quad . \quad . \quad (12)$$

In order to evaluate the equations expressed by (10), (11) and (12), it is first necessary to find the magnetic intensity vector H with the aid of Eqt. (9). This cannot be done with the formula as it is expressed by (9) because the method of notation is not dependent upon the coordinate system used for solving the problem. This difficulty may be overcome in two steps by first using rectangular coordinates and then transforming to the most convenient coordinate system for the particular problem under consideration. For the rectangular coordinate system, let:

$$r = x\,i + y\,j + z\,k \quad . \quad . \quad . \quad . \quad . \quad (13)$$

$$dl = d\,X\,i + d\,Y\,j + d\,Z\,k \quad . \quad . \quad . \quad (14)$$

$$\rho = (x - X)\,i + (y - Y)\,j + (z - Z)\,k \quad . \quad . \quad . \quad . \quad . \quad . \quad . \quad . \quad (15)$$

By substituting equations (14) and (15) in (9), the three mutually perpendicular components of H are obtained. Since the integration of (9) is performed along a curve in space, the coordinates X, Y and Z can be expressed in terms of a single parameter m, and thereby reduce Eqt. (9) to the forms:

$$H_X = \int_{m_0}^{m_1} f_1\,(m)\;dm \quad . \quad . \quad . \quad . \quad . \quad (16)$$

$$H_Y = \int_{m_0}^{m_1} f_2\,(m)\;dm \quad . \quad . \quad . \quad . \quad . \quad (17)$$

$$H_Z = \int_{m_0}^{m_1} f_3\,(m)\;dm \quad . \quad . \quad . \quad . \quad . \quad (18)$$

As a basic arrangement and a first approximation to a single turn coil around a large diameter load, consider

(*Continued on page* 28A)

Fig. 15. Magnetic field intensity in a conducting sheet of material under a two-conductor work-coil.

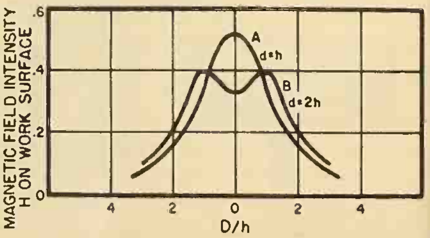

An AMPLIFIER for MAGNETIC OSCILLOGRAPHS

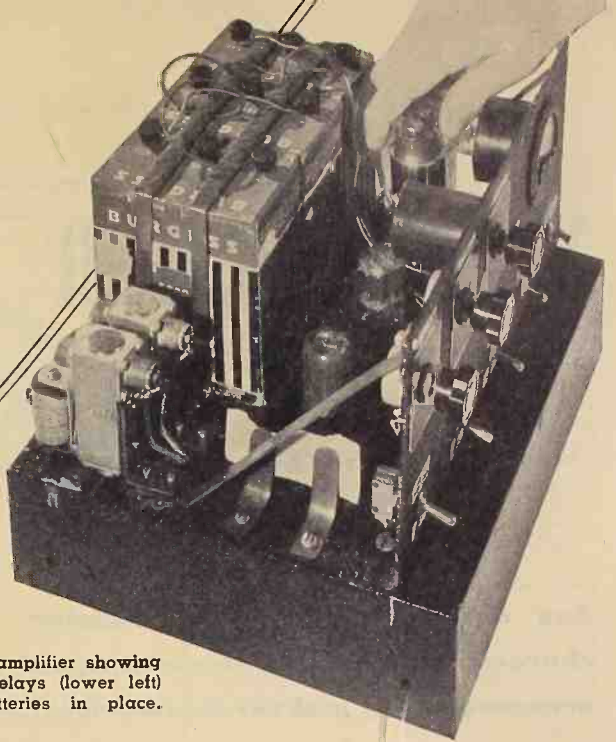

Top view of amplifier showing the coaxial relays (lower left) and the batteries in place.

By C. J. TIRK
Engineering Laboratories
Westinghouse Electric Corp.

Design of a 3-stage transformerless amplifier having a high impedance input and a low impedance output.

BUT FOR ONE major limitation — low input impedance — the magnetic oscillograph would have a much wider field of application. It could, for example, be used to record voltages appearing at potential taps of condenser bushings, a use for which it is ideally suited, but for its one drawback. The advent of a new amplifier, which offers the necessary high impedance input, will undoubtedly extend the utility of the already useful magnetic oscillograph.

By the use of this amplifier the field of the magnetic oscillograph is extended to include many measurement problems confronting utility and industrial engineers. In addition to the application mentioned above, utility engineers could use the oscillograph for such thing as recording voltages at the potential taps of carrier-current coupling devices; engineers in industry can find a multitude of new uses, such as in recording the operation of electronic devices.

The magnetic oscillograph is primarily a recording device. It can make multiple, simultaneous records, and is well adapted to measurements of transient phenomena. The frequency response of the magnetic oscillograph extends from d.c. to several thousand cycles per second, which range is adequate for many important measurements.

Without modifying any of these desirable characteristics, the new amplifier, which has an input impedance of 10 megohms, removes the impedance limitation. This condition permits the use of the oscillograph with various forms of capacitance voltage dividers, as well as making possible a performance record of electronic control systems and servomechanisms, with no more burden on the circuits than would be imposed by a vacuum-tube voltmeter.

The new amplifier has three stages (see Fig. 1A). The input and output stages are cathode coupled to give high input and low output impedances, and the second stage is plate coupled to provide voltage gain. Twin triodes are used throughout. The double input is so arranged that the difference of two voltages that are above ground potential can be measured, with the amplifier chassis and power supply grounded.

A separate amplifier is required for each oscillograph element. Within the frequency range of the oscillograph, the amplifier distortion, including phase shift, is negligible. The over-all sensitivity of the amplifier-oscillograph combination depends in part, of course, on the oscillograph sensitivity. With a high-frequency-response element, the sensitivity is about three volts per inch; with a high-sensitivity element, it is about 0.06 volt per inch.

Because most tests in which the amplifier is used are staged, or are of such a nature that the device is self-calibrat-

(*Continued on page* 25A)

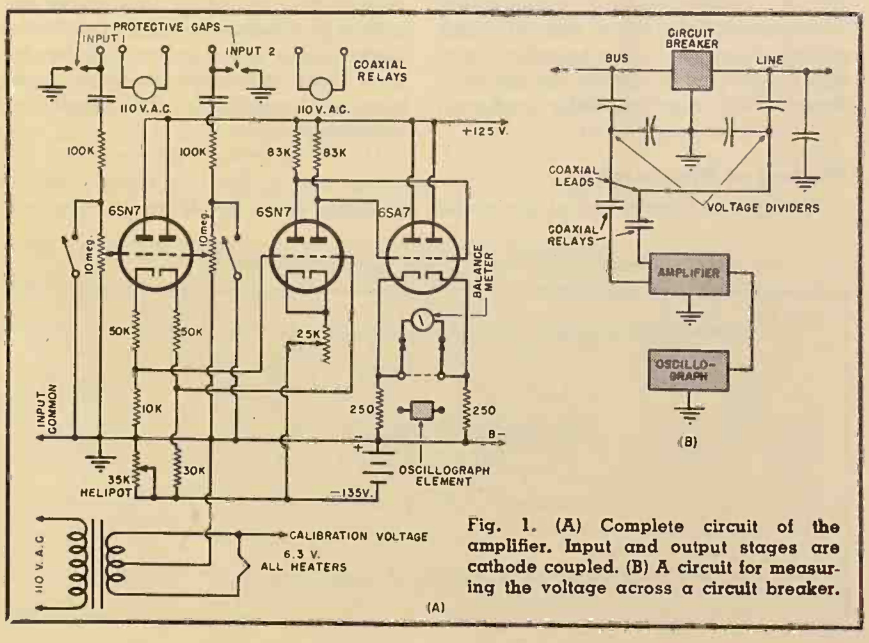

Fig. 1. (A) Complete circuit of the amplifier. Input and output stages are cathode coupled. (B) A circuit for measuring the voltage across a circuit breaker.

The MONOFORMER

By
ALLEN C. MUNSTER
Research Div., Philco Corp.

Any desired single-valued transfer characteristic may be obtained to an accuracy of 1 % with the monoformer.

Fig. 1. Typical monoformer tubes. The transfer characteristics may be seen on the aluminum discs at the ends of the tubes.

THE MONOFORMER is an electronic cam. By all-electronic methods it can provide any desired single-valued transfer characteristic. Voltage and impedance levels employed are those common to electronic systems, and power requirements are small. The monoformer employs a small electrostatic cathode-ray tube containing a target plate carrying the desired transfer characteristic, and a simple feedback network. For many applications the feedback network contains no components other than a single resistor.

With regard to accuracy and response time the monoformer compares favorably with electromechanical devices used to develop nonlinear relationships. The monoformer has excellent transient response, reaching its final output within 3 microseconds after a step of input voltage is applied. The transfer function is accurate to within one per-cent. Repeatability is substantially unaffected by tube aging and the like.

Method of Operation

The various components of the monoformer are shown in Fig. 4. The gun structure of the monoformer tube is conventional. An additional anode is included to collect secondary electrons from the target plate used to replace the phosphor. This target plate consists of an aluminum disk printed with carbon ink. As shown in Fig. 3, the desired law of the monoformer forms the boundary between the uncoated and carbon-coated areas of the target disk.

The monoformer shown in Fig. 4 operates by servoing the electron beam to the boundary between the aluminum and carbon areas of the target plate. Aluminum and carbon have different secondary emission ratios. Consequently the target current is a function of the material struck by the electron beam. A voltage determined by this target current is fed back to one set of deflection electrodes in such a sense that the electron beam is caused to move to the boundary separating the coated and uncoated areas.

If the boundary between the two areas is $y = F(x)$, y signals may be obtained from the deflection electrodes in the feedback loop, while the independent x signal is applied to the other set of deflection electrodes. The monoformer does not introduce any active loading or extraneous signals into the input signal bus.

Fig. 2. Block diagram of a polynomial generator.

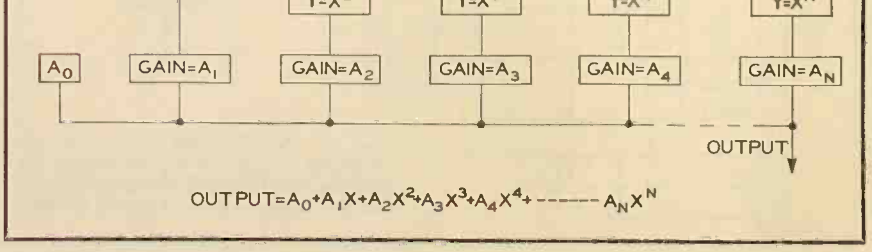

Transient Response

The monoformer behaves like a proportional servo system when the frequency response around the feedback loop is adequate. However, very high frequency feedback signals can be required by either high frequency input signals or transfer functions having steep slopes. In either case the electron beam may be driven completely onto one of the target areas, and the system temporarily acts as a regulator rather than a servo. The dead zone of the conventional regulator is replaced by a servo zone in the monoformer. The damping provided by the servo zone prevents instability although a small overshoot may occur. Analysis shows that the monoformer with no more than one stage of amplification in the feedback loop is always stable.

Transient response may be improved by increasing the figure of merit of either the feedback amplifier or the monoformer tube. (Transconductance of the monoformer is $\delta I_{target}/\delta E_{deflection}$ as the electron beam crosses the boundary between the target areas.) Increase of the monoformer transconductance much beyond its present value of 40 micromhos requires either an improved secondary emission surface or redesign of the electron gun to increase the current density of the beam.

Push-pull feedback provides better transient response than does single-ended feedback because the deflecting voltages add but the time constants associated with the deflection plates do not. Furthermore, push-pull feedback provides greater accuracy.

Accuracy

The monoformer electron beam cannot track the target curve exactly, but must produce an error signal to effect deflection of the beam to the curve. This "static error" can be reduced by increasing the gain around the feedback loop. If an amplifier is employed in the feedback network, it may limit at output voltages above that required for the peaks of the monoformer law without affecting static accuracy. However, limiting in the feedback amplifier will impair the transient response.

If sufficient gain is provided around the feedback loop, accuracy of the monoformer is limited mainly by aberrations in the electron beam, but some error is caused by astigmatism if single ended deflection is employed. Errors are largest when the law of the monoformer has corners which are too sharp for the beam to resolve.

Applications

The monoformer may be used wherever a nonlinear relationship is required. Its major uses to date have been:

1. Analog computers, where the relationship $y = f(x)$ is used to modify an input voltage for computational purposes.
2. Volume compressors and expanders, to increase the efficiency of transmission systems.
3. Waveform generators, where the input signal, x, may be a sawtooth or sine wave, and the output signal, y, is the waveform desired.

Targets for these applications are illustrated in Fig. 3. The clipper-limiter shown may be used as either an "infinite-clipper" (deflection to left of center of target), or as a linear amplifier with a sharp limiting threshold (deflection to right of center of target).

In many analog computer applications it is desirable to alter the relationship $y = f(x)$ for different problems. If the number of different relationships required is small, separate monoformer tubes may be employed. However it is not necessary to obtain a new monoformer for each relationship. The outputs of several monoformers may be added to obtain new functions as shown in Fig. 1 where a number of monoformers of the form $y = x^n$ are used to generate an arbitrary polynominal of the form $y = \Sigma_n\ a_n x^n$. By replacement of the monoformers with those of the form $y = e^{nx}$ or $y = \cos nx$, the same generator may be used to generate $y = \Sigma_n\ a_n e^{nx}$ or $y = \Sigma_n\ a_n \cos nx$. Such a machine can be used to solve many of the time consuming equations confronting the engineer.

Construction of the Monoformer

The gun structure of monoformer is that of a standard electrostatic cathode-ray tube, except that the grid-cathode spacing is less than that usually found in tubes which employ intensity modulation. This smaller spacing permits increased beam current, but makes cut-off more remote. Since the monoformer tube is not generally intensity modulated, cut-off is unimportant.

The target is a one inch diameter aluminum disk with the law of the monoformer printed in carbon ink. Printing is done from a photoengraving made from a larger drawing. This process prevents the introduction of errors between the large, easily checked drawing and the final product.

Two monoformer tubes are shown in Fig. 1. The tubes are 8 inches long and 1¾ inches in diameter. Standard CRT bases are employed. Connections to the target and collector electrode are made by conventional CRT high voltage connectors. In the tubes shown, the collector electrode was made transparent to permit easier observation of the target. The target is usually dusted lightly with phosphor to assist in initial adjustment of the monoformer.

Operating Conditions

Typical operating conditions for the monoformer tube without amplification in the feedback loop are given in Table I. Both positive and negative voltages are applied to the tube so that the signal from the target may be d.c. coupled to the deflection plates without introducing any distorting fields between the deflection plates and the second anode.

If an amplifier is used in the feedback loop, the collector may be connected to the second anode and the target operated with negative bias. The plate voltage required for the amplifier tube then serves to bring the average feedback signal level applied to the deflection plates to the same potential as the second anode. With suitable amplification in the feedback loop, the response time may be decreased to 1 μsec. without loss of accuracy.

* * *

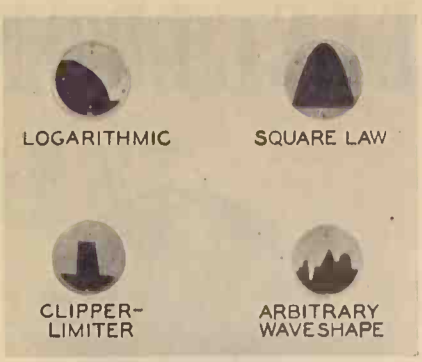

Fig. 3. Typical monoformer targets. The targets are made of aluminum and the dark portions, constituting the desired wave shape, are printed with carbon ink.

Accelerating Voltage	—500 volts
Accelerating Current	400 microamperes (including centering controls, etc.)
Second Anode Voltage	0 volts
Collecting Voltage	100 volts
Collecting Current	50 microamperes
Signal Input	40 volts for full deflection
Signal Output	30 volts for full deflection
Accuracy	1%
Response Time	400 μsec. to step input

Table I. Typical operating conditions for the monoformer tube without amplification in the feedback loop.

Fig. 4. Details of the interior construction of a printed target monoformer tube. The gun structure is similar to that of a standard electrostatic cathode-ray tube.

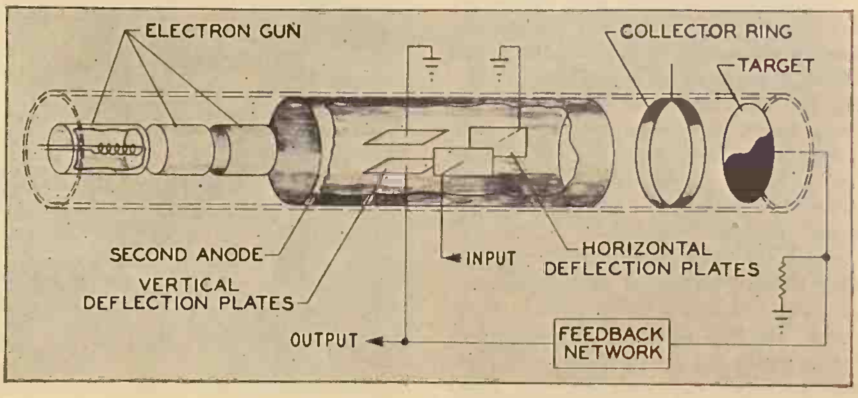

ELECTRONIC FLUORESCENCE DETECTOR-COMPARATOR

By CHARLES WEEKS

Technical Director
Menlo Research Laboratory

Fig. 1. Operator is shown making a routine laboratory comparison.

This instrument, called a Fluoretor, provides an ultraviolet light source powered by flashlight batteries. It features an integral dark chamber.

ULTRAVIOLET light sources of various kinds have been widely applied in the commercial detection and identification of materials such as ores, minerals, chemicals, food contaminants, and the like. Materials-testing engineers use u-v for non-destructive fluorescent examination of parts and structures for manufacturing defects or incipient strain failures.

Criminologists utilize such equipment for discovery of clues, for comparison and identification of fabrics, dusts, and stains of many kinds as well as for tracing the movement and handling of objects which have been treated in such a way as to leave fluorescent markings on the hands of people touching them. Altered documents, postage stamps, gems, and a tremendous variety of items yield valuable information under ultraviolet. In medical fields, diagnosis of certain skin infections such as ringworm, and measurement of blood circulation (with the use of fluorescent tracing materials injected into the blood stream) are two of many possible uses.

A recent development of Menlo Research Laboratory, Menlo Park, California, permits the application of u-v to such operations without the limitations imposed by power lines, heavy batteries, and high ambient light levels. The instrument, called a Fluoretor, is illustrated in use in Fig. 1, making a routine laboratory comparison.

The specimens being examined are enclosed within the light-tight cylindrical housing in the technician's left hand. Complete self-contained power supply is housed in the barrel of the handle which is attached by a knuckle joint to the light-source and filter housing. The specimens are studied under a three-power magnifying eyepiece which slides in and out for focusing. The end cap of the dark-chamber housing is a slip fit and a set of six caps is provided for securing various kinds of samples for observation.

Specimens too large for insertion in the chamber can be inspected by holding the open end of the dark-chamber against their surfaces. For irregular surfaces, a soft-sponge-rubber cone fits this end of the unit and excludes ambient light under the area under study.

An exploded view of the instrument is shown in Fig. 2. Connections between

(*Continued on page* 29A)

Fig. 2. Exploded view of the Fluoretor shows the various parts used in its construction. Note the flashlight batteries used as a power source.

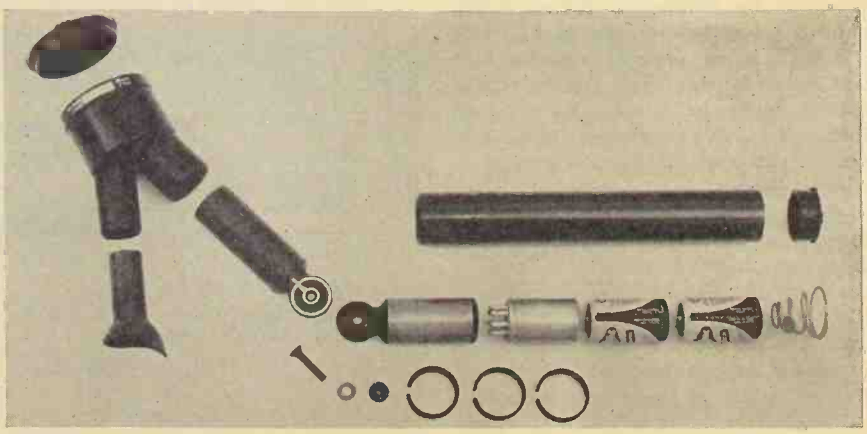

RADIO NAVIGATION EQUIPMENT

By JOHN P. GRIFFIN
Northwest Airlines, Inc.

Dual accessory unit for VOR navigation system.

The second and concluding part includes a detailed analysis of the various portions of a VOR system.

THE FAIRLY complete analysis of the Visual Omni-Range instrumentation and circuitry which follows is intended to give the reader a comprehensive, over-all picture of the functioning of the system.

VOR Instrumentation

A functional diagram of the instrumentation system appears in Fig. 1. The system provides the following facilities:

a. Localizer, tone type, for the reception of ILS signals.

b. Localizer, phase type, for reception of ILS signals from phase type localizers which are expected to come into general use because of their improved accuracy and other advantages. The transmission system is practically identical to the system of VOR transmission.

c. Omni-Directional Range reception, combining ADF and magnetic compass information on the Radio Magnetic Indicator.

d. Omni-Directional Range reception with course information presented on the ILS Deviation Indicator.

Receiver

Channel selection is made from the cockpit by use of a control which permits a choice of any one of 280 channels over a nine-wire system. The coarse frequency dial may be set to any one of ten positions and the fine frequency to any one of 28 positions.

A mechanism, designated the Autopositioner, drives either the megacycle shaft or the tenth megacycle shaft from a single motor through a pair of simple overrunning clutches and stop mechanisms.

The receiver is a double conversion superheterodyne having a tunable first i.f. of 19.5-21.4 mc. and a second fixed i.f. of 3.2 mc. Refer to the block diagram of Fig. 3.

When used with the accessory unit for complete instrumentation the receiver provides for both track flying by means of a radial selector (Omni-Bearing Selector) and a deviation indicator and for ADF flying by means of the RMI.

Fig. 1. Functional block diagram of the VOR instrumentation system.

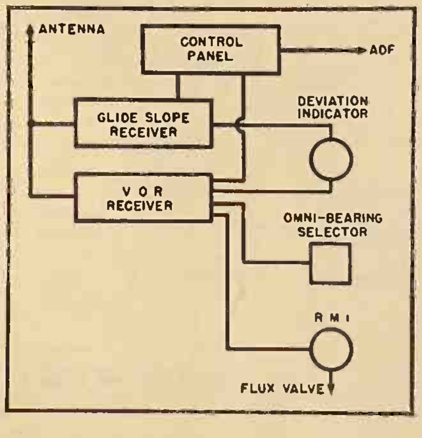

The accessory unit houses two dynamotors, the servo amplifier for the RMI and the Omni-Bearing Indicator. Since the unit is mounted in the radio rack, the bearing indicator is not used by the pilot. For that reason the unit will get scant attention in this article. It is not shown on Fig. 1; however, the indicator portion of the accessory unit is shown in other schematics where its function is pertinent to the operation of other circuits.

The receiver also serves as an ILS localizer receiver and may be used as a v.h.f. communications receiver by providing the proper type antenna. (V.h.f. communication signals are vertically polarized, Omni-range and localizer signals horizontally polarized.)

A switch on the Omni-Bearing Selector selects either tone or phase modulated localizer signals. An audio volume control is located on the Radio Control Panel.

Primary supply is 28 volts d.c. from the ship's bus and 26 volts, 400 cycles from the ship's inverters. Tube types CK5654/6AK5 and 5670 are used throughout the unit except one 0A2 voltage regulator.

Fourteen crystals supply the injection frequencies for the first converter. They are selectable by the tap switch driven by the megacycle autopositioner. As is indicated in the block diagram of Fig. 3, the megacycle positioner also tunes the crystal multiplier string as well as the four tuned circuits in the r.f. amplifier preceding the first converter.

Injection frequencies for the second converter are supplied by a group of 20 crystals and are selected by a switch driven by the tenth megacycle autopositioner. This positioner simultaneously tunes the second injection crystal multiplier circuit as well as the four tuned circuits associated with the first i.f. amplifier string.

Signals received in the selected 2 mc. band pass through a pair of tuned

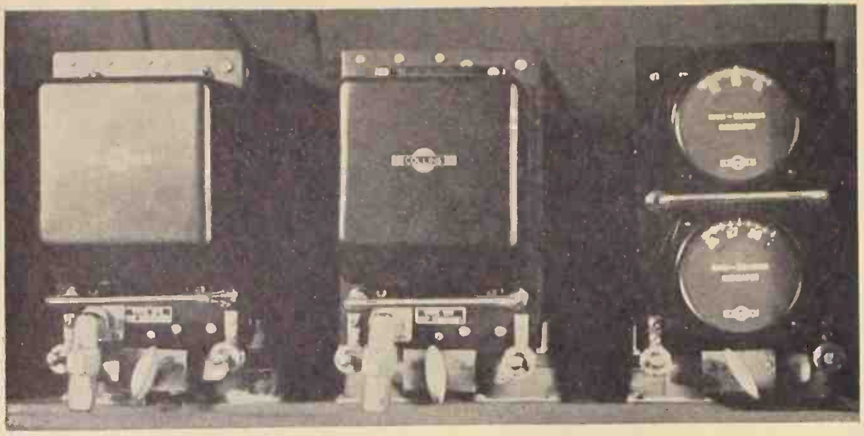

VOR installation in NWA aircraft—two receivers, one dual accessory unit.

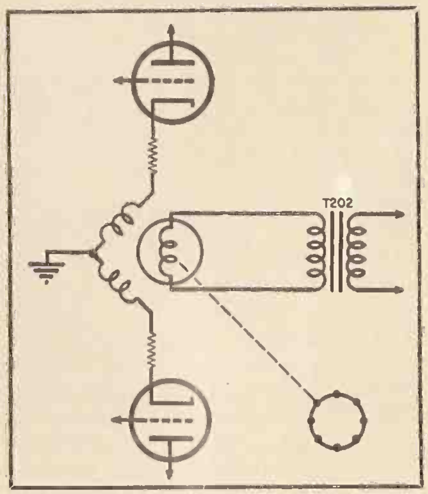

Fig. 2. Typical resolver circuit.

circuits to the first converter. Also feeding the first converter is an injection voltage of suitable frequency to heterodyne the signal down to a frequency lying within the 19.5-21.4 mc. band of the first i.f. strip. This first amplifier is tuned to the specific frequency desired and it is thereby selectively amplified. It is then fed to the second frequency converter where it mixes with an injection voltage obtained from the second crystal group. The output of the second frequency converter lies in the middle of the 3.2 mc. second i.f. amplifier pass band and is selectively amplified and passed to the detector.

Rejection of adjacent channel signals is provided by the selectivity of the second i.f. which operates at 3.2 mc. Added to the selectivity of the first i.f. an over-all rejection of 70 db. to adjacent channel signals is obtained.

Accurate operation of the indicator system requires a constant signal output which is obtained by the use of a d.c. amplifier in the a.v.c. system. A combination oscillator and rectifier is used to provide the negative voltage supply for the d.c. amplifier circuit and for other bias applications.

There is nothing unusual about the detector. It includes a peak clipping type noise limiter. A tap on one of the frequency selector wafers in the receiver selects the proper audio gain setting for 30 per-cent modulated voice signals emanating from navigation facilities and 100 per-cent modulation signals delivered by communication stations. The level switching, combined with the inherent leveling action of the noise limiter, insures close control of audio output at the proper preselected level.

Indicating System

Illustrated in Fig. 6 are the facilities for the operation of the Omni-Range and localizer indicating system. The RMI, which combines the magnetic and Omni course information, is a separate instrument unit but is controlled by a servo amplifier which is an integral part of the radio receiver.

Voltage from the detector feeds through an amplifier into a 10 kc. filter and thence through an additional amplifier to an FM discriminator where the reference phase is removed from the 10 kc. subcarrier. The modulation frequency is then passed through a phase splitting network and amplifier to the two quadrature field coils of a resolver which forms part of the Omni-Bearing Selector. From the resolver the voltage is fed through an amplifier and phase detector to the vertical needle of the deviation indicator. Immediately ahead of the 10 kc. filter, voltage from the detector is taken off and passed through a 30 cycle filter from which the 30 cycle variable phase voltage emerges. After amplification and phase detection it has the characteristics necessary to the operation of the deviation indicator. This portion of the circuit provides for deviation indicator flying of any preselected radial.

The TO-FROM indicator on the Omni-Bearing Selector is an auxiliary indicator. It indicates TO when the aircraft is on course and headed toward the station. It indicates FROM when the aircraft is on course and headed away from the station. It moves to the center position when either the reference or the variable signal falls below a safe value.

Operation of the TO-FROM indicator is through a phase detector which is combined with the phase detector operating the course needle of the deviation indicator. In order to properly control the indicator, it is neces-

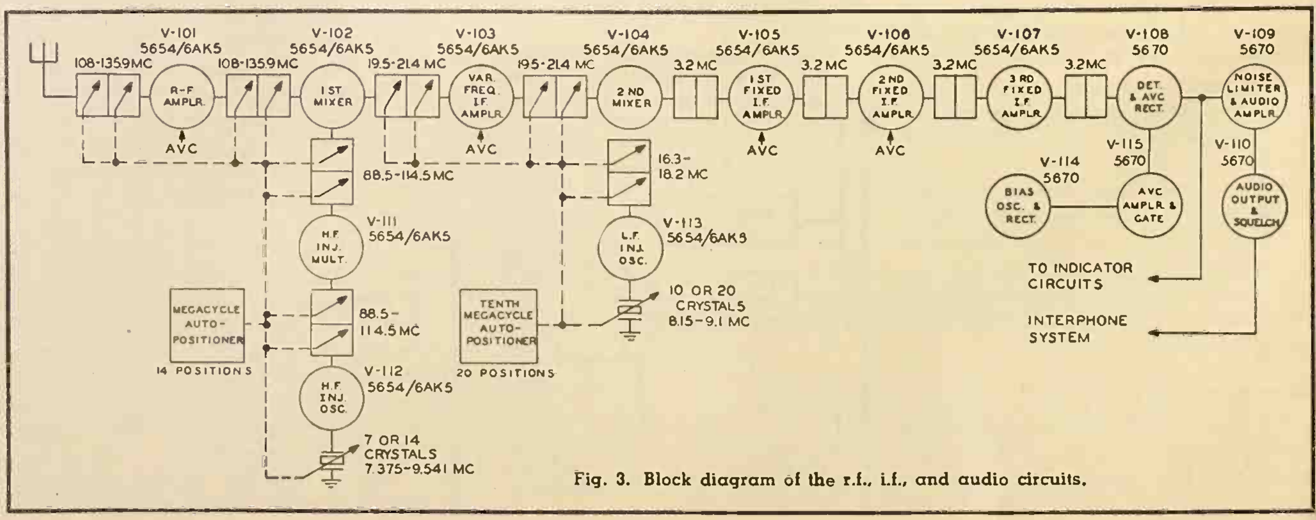

Fig. 3. Block diagram of the r.f., i.f., and audio circuits.

sary to shift the phase of the variable voltage entering this second detector through an angle of 90 degrees. This means that the indicator will show the pilot which side of the station he is on and will swing from TO (correct reading) to FROM (incorrect reading) if the aircraft crosses a course line 90 degrees displaced from the selected course.

At a position due south or due north of the station there would be no phase difference and the resultant, fed to the deviation indicator, would keep the needle centered. At any other position of the aircraft the needle would show a deflection. If the manual phase shifter (Omni-Bearing Selector) is manipulated to bring the needle back to zero, it will then read in degrees the circular distance it was moved, which is the phase difference or the azimuth position of the aircraft. Now if the pilot flies to keep the needle centered he will maintain a constant phase difference and will be flying a radial to the station.

Circuits

Refer to the block diagram of Fig. 3. In position one of the frequency selector, the r.f. amplifier and its tuned circuits pass all frequencies between 108 and 110 mc. A band 2 mc. wide appears in the first frequency converter. In this position, the injection into the first converter is exactly 88.5 mc. The 88.5 mc. injection frequency can beat with anything in the 2 mc. range and produce any number of i.f. frequencies. The following i.f. stage, however, is tuned exactly to a tenth of a megacycle. If it happens to be tuned to 19.5 for example, that will be the strongest beat frequency passed and for all practical purposes, the only frequency appearing at the control grid of the second converter. Since the above mentioned high i.f. stage tuning is ganged to the crystal selector and the oscillator tuning is ganged to the crystal selector, only one frequency is injected, via the cathode, into the second converter, namely 16.3 mc. The difference frequency is 3.2 mc., which is the fixed intermediate frequency. Had the high i.f. amplifier been tuned to any of the other frequencies presented to it by the first converter, then the new frequency, upon entering the second converter, would mix with a new injection frequency to produce 3.2 mc. For example, if the high i.f. amplifier is tuned to 19.8 mc., the autopositioner will at the same time shift crystals and tune the second oscillator to 16.6 so that these are the two frequencies entering the mixer. Their difference, 19.8-16.6 is 3.2, the fixed i.f.

Refer to Fig. 7. The signal from the third fixed i.f. stage is detected in the right hand section of the diode-connected tube V_{108}. The left hand section of V_{115} is a d.c. amplifier for a.v.c. The right half is used as an a.v.c. gate.

The diode load resistor for the a.v.c. detector is R_{134}. There will be no drop across R_{134} while the input to the diode is zero. It can be seen from an inspection of Fig. 4 that when the no-input condition prevails, there is no potential difference between grid and cathode of V_{115}, the a.v.c. amplifier. Since there is a positive voltage on the plate, current will flow through R_{114}, R_{137}, R_{136}, R_{135} and the tube. The current flow through the resistor string is sufficient to nullify the bias voltage from V_{114} (connected between R_{136} and R_{137}). One triode section of V_{114} operates as an oscillator and the other section, connected as a diode, rectifies the oscillator output. The d.c. thus obtained is applied between R_{136} and R_{137}. This action places both cathodes of V_{115} above ground potential. The gate section will be cut off due its positive cathode. Hence no signal input to the a.v.c. detector results in a closed gate.

A signal input to V_{108} will result in a drop across R_{134}. This drop will bias the a.v.c. amplifier, V_{115}, to near cut-off. With little or no current flowing in the resistor string, R_{114}, R_{137}, R_{136}, and R_{135}, the bias applied from V_{114} becomes effective in making the cathodes of V_{115} negative. The gate section of V_{115} now has a negative cathode and will conduct, resulting in a.v.c. output voltage which is applied to the control grids of four of the r.f. and i.f. amplifier tubes.

In the same schematic, Fig. 7, the right hand section of V_{109}, the first audio stage, is biased to cut-off when no modulated signal is being received and is allowed to conduct when the input contains a modulated signal. The cut-off bias is developed by the right sec-

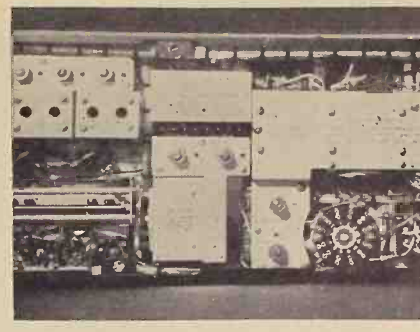
Collins 51R v.h.f. navigational receiver.

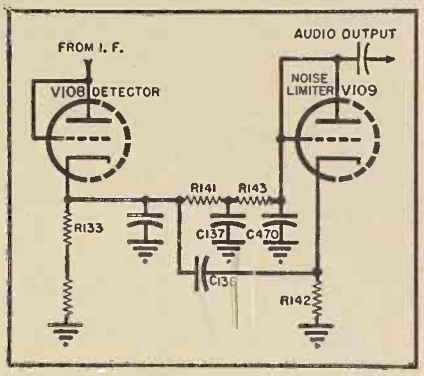

Fig. 4. Circuit of the noise limiter.

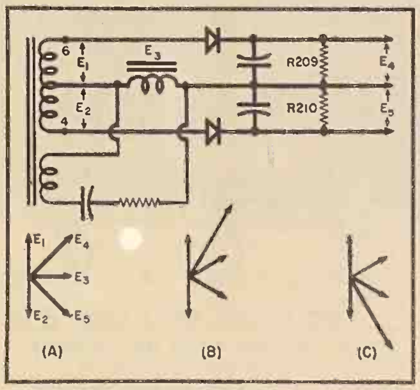

Fig. 5. Discriminator circuit and operation.

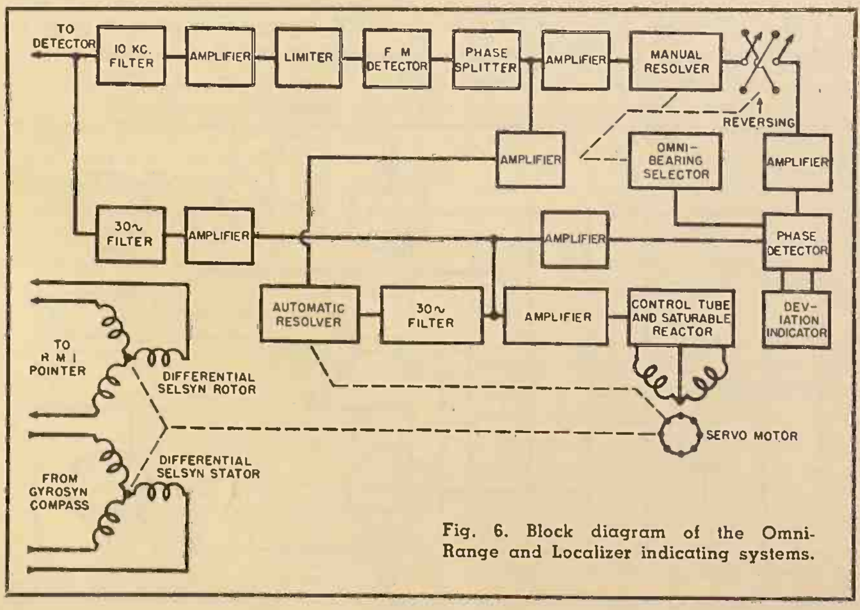

Fig. 6. Block diagram of the Omni-Range and Localizer indicating systems.

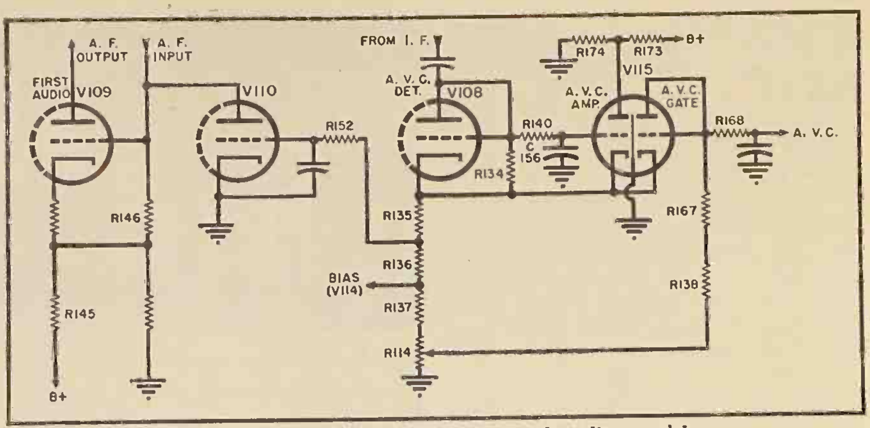

Fig. 7. Circuit of the detector, a.v.c., and audio squelch.

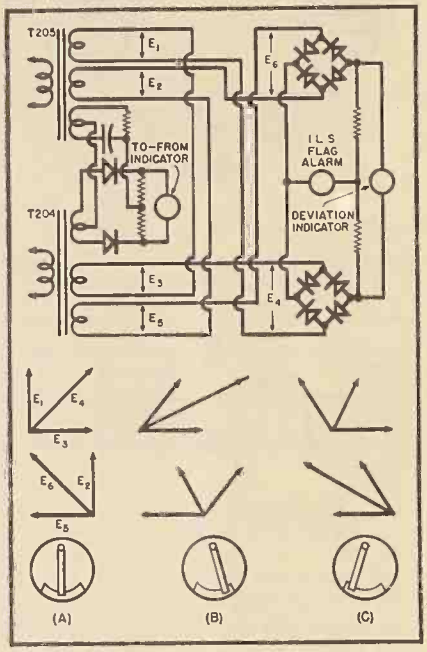

Fig. 8. Deviation circuit and operation.

tion of V_{110} whose grid is connected to resistor string R_{135}, R_{136}, R_{137}, and R_{114}. As previously explained, when there is no signal input, the a.v.c. amplifier is conducting and as a result there is a positive voltage developed at the junction of R_{135} and R_{136}. Since V_{110} is connected to this point, the tube is conductive and its current flow develops a voltage across R_{146} which is applied to the grid of V_{109}. Being thus biased to cut-off, V_{109} does not conduct when there is no signal input. When a signal appears, the drop across R_{134} cuts off V_{115} and with no current flowing through R_{135} and R_{136}, the bias from V_{114} predominates at the junction of these resistors. This negative voltage cuts off V_{110} and with the cessation of plate current through R_{146}, V_{109} is no longer biased to cut-off.

As shown in Fig. 4, the noise limiter is connected to the cathode of the detector. The positive audio pulses thus derived are straightened out by the filter network through which they are passed and applied to the diode plate (V_{109}). This positive voltage on the diode plate enables the tube to conduct. Since the cathode of the diode is connected to the same signal source through C_{136}, tube conduction varies at an audio rate. Any sharp noise pulse will not appear on the plate because of the smoothing action of the filter but will appear as a positive pulse on the cathode and bias the tube to cut-off. Since recovery time is practically instantaneous the gap thus produced in the continuity of the audio is not noticeable.

Refer to Fig. 5. The voltage across terminals 4 and 6 is rectified in the crystal diodes and appears at the load resistors R_{209} and R_{210}. The voltage across the third winding is applied to the choke in the center leg. This third winding is series resonant at 9960 cycles with the condenser shown and will therefore apply its maximum voltage across the choke when the primary frequency is 9960 c.p.s. As shown in vector diagram A, this voltage is 90 degrees out of phase with the voltages appearing across the load resistors. As the primary voltage swings to its 480 cycle maximum in one direction this phase changes as shown in vector diagram B. As it swings in the opposite direction the phase of E_3 reverses. Since this swing occurs at a rate of 30 c.p.s. the demodulated 30 cycle voltage is delivered to the output.

Instruments

The input to the indicating system contains the reference and the variable signals. It is the phase difference between these signals which indicates aircraft position and which operates the deviation indicator. In passing through the upper branch of the diagram shown in Fig. 6, the reference phase is removed from the 10 kc. subcarrier, is demodulated and presented to the manual resolver which is part of the Omni-Bearing Selector. This resolver, actuated by the previously mentioned knob on the right side of the instrument, reduces the phase shift between reference and variable signals to zero and shows in the window the angular difference between the two voltages.

Besides going to the manual resolver, the reference voltage is also fed to the automatic resolver. Assume for the moment that there is zero phase shift (null position) through this resolver. The resolver output following a 30 cycle filter is mixed with the variable phase voltage and fed to a phase sensitive amplifier. Under the no-phase-difference condition there will be no output from the amplifier and no torque on the servo motor. Should the aircraft now change its position to a point where there is a difference in phase between reference and variable signals, the output of the phase sensitive amplifier will drive the servo motor. Since the rotor of the automatic resolver is connected mechanically to the same shaft as the rotor of the servo motor, it also turns and moreover will turn in the direction necessary to reduce the phase angle. Obviously the motor will stop turning when the phase angle

(*Continued on page* 31A)

Fig. 9. Resolver feed circuit with vector diagram of operation.

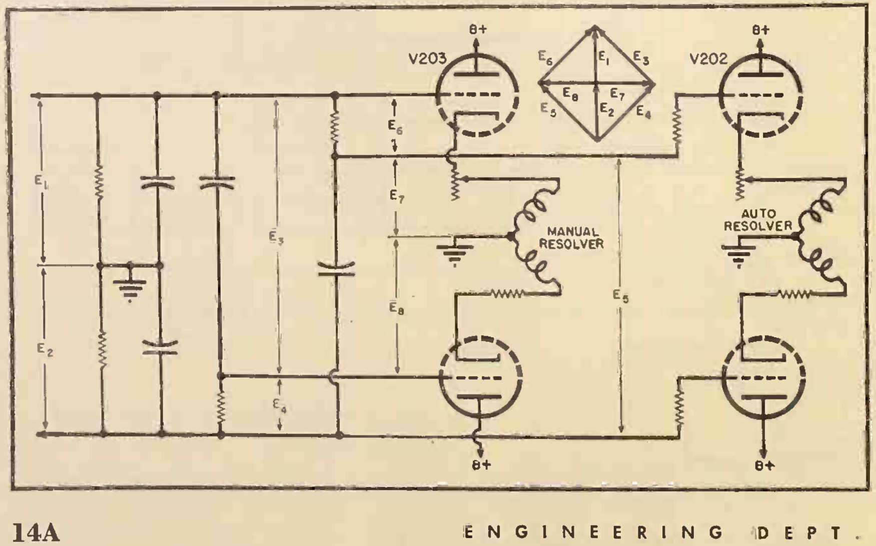

MICROWAVE ANTENNAS

By
J. RACKER
Federal Telecommunication Labs.

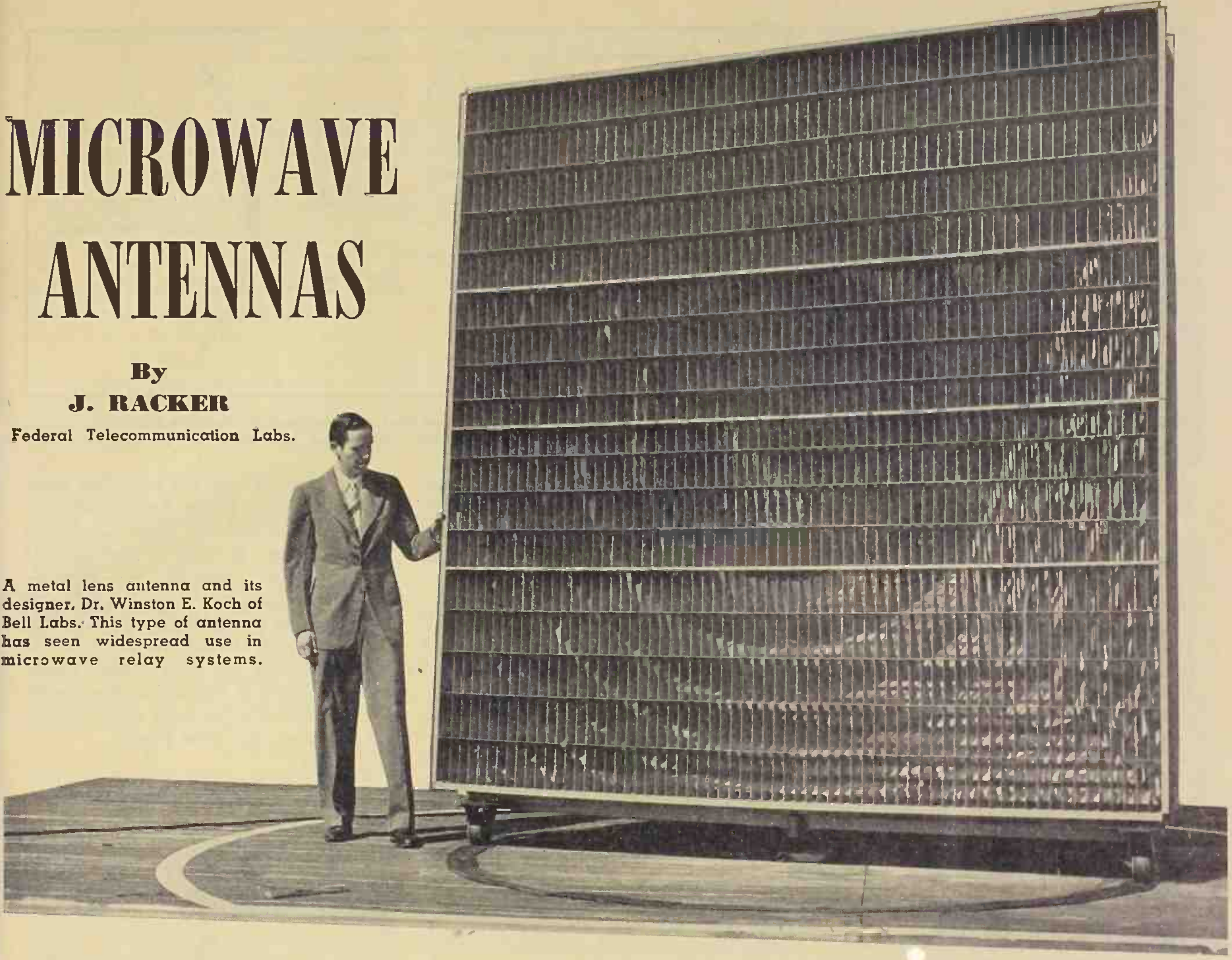

A metal lens antenna and its designer, Dr. Winston E. Koch of Bell Labs. This type of antenna has seen widespread use in microwave relay systems.

A discussion of such factors as directivity and gain for the three most important microwave antenna types—parabolic, horn, and lens antennas.

THE ability to achieve a high degree of directivity with simple, inexpensive antennas is by far the most important reason for the expanded use of microwave equipment. The directivity or power gain that can be attained is best illustrated by noting that a 1 watt, 2000 megacycle system using 10-foot parabolic antennas for both transmitting and receiving provides equivalent service to a system using dipole antennas and an output of about 1,000,000 watts. Because of this factor, it has become more economical in many areas to use radio links for television and communication relaying purposes than equivalent wireline circuits. Furthermore it is readily conceivable that in the future a large portion of inter-city telephone facilities will be effected through the use of microwave links.

There are many types of antennas that have been developed, particularly for radar applications. Most of these are modifications of three basic types, namely, parabolic, horn, and lens antennas. It is far beyond the scope of this article to cover all of the many types and discussion will be confined to the three aforementioned types. In some texts covering this subject, antenna arrays are described; however, the author has defined[3] the lower limit of microwaves at 900 mc., at which frequency arrays are rarely used.

There are two terms frequently employed to describe the characteristics of microwave antennas. One, the power gain, determines the effectiveness of the antenna for transmitting purposes.

Fig. 1. Electromagnetic horn.

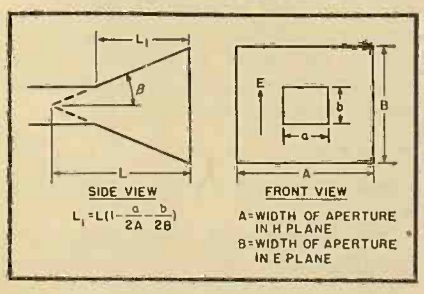

The power gain of a microwave antenna is given by:

$$G = \frac{P}{P_0} = 10 \log_{10} \frac{P}{P_0} (\text{db}) \quad . \quad . \quad (1)$$

where P is the power flow per unit area of the transmitted electromagnetic wave at some distant point in the direction of maximum radiation, and P_0 is the power flow per unit area at that same point which would have been produced if all the power were radiated equally in all directions (isotropic antenna). (Note that comparison is made with respect to isotropic rather than dipole antenna).

The second parameter, the effective area, is a qualitative measure of the ability of the antenna to collect power at the receiver. The effective area of a receiving antenna is defined by the following expression:

$$A = \frac{P_r}{P_0'} \quad . \quad . \quad . \quad . \quad . \quad . \quad . \quad . \quad (2)$$

where P is the received power available at the antenna terminals, and

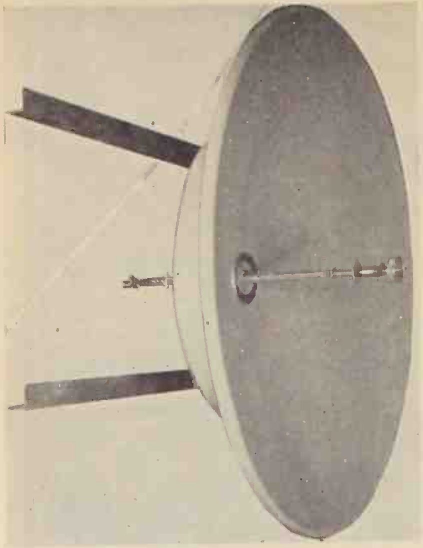

Fig. 2. Circular parabolic antenna.

P_0' is the power per unit area of the incident wave.

It can be shown that there is a constant relationship between gain and effective area of an antenna. The ratio G/A, furthermore, is the same for all types of antennas and is equal to:

$$\frac{G}{A} = \frac{4\pi}{\lambda^2} \quad . \quad . \quad . \quad . \quad . \quad . \quad . \quad . \quad (3)$$

From Eqt. (3) the gain of an antenna can also be defined as:

$$G = \frac{4\pi A}{\lambda^2} \quad . \quad . \quad . \quad . \quad . \quad . \quad . \quad . \quad (4)$$

Fig. 4. Radiation pattern of (A) isotropic antenna and (B) directive antenna.

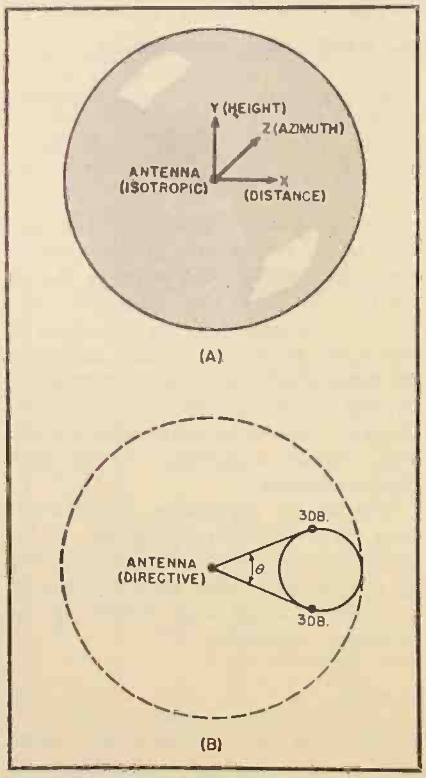

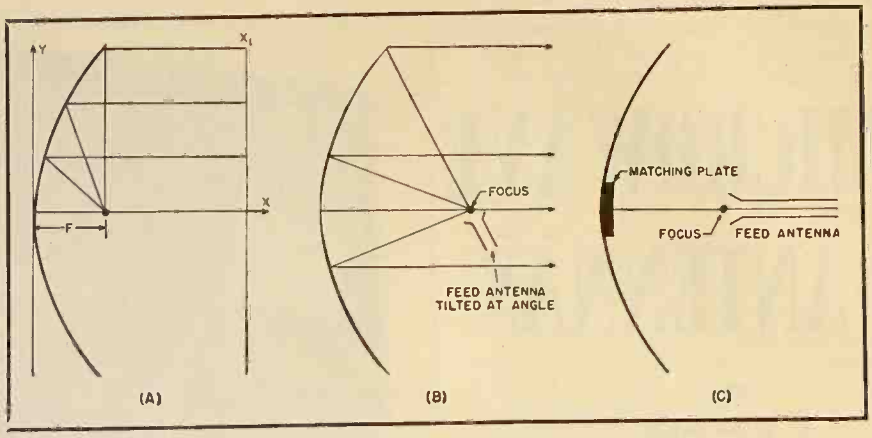

Fig. 3. (A) Parabolic curve. (B) Offset feed antenna used to minimize shadow. (C) Matching plate for improving impedance matching of parabola.

It should be noted that Eqt. (3) applies only when the antenna and wave polarizations are the same. For the case where they are not, the gain is given by the equation:

$$G\alpha = G\cos^2\alpha \quad . \quad . \quad . \quad . \quad . \quad . \quad . \quad . \quad (5)$$

where α is the angle between plane of polarization of the antenna and the incident field.

Power gain is achieved because the antenna concentrates the available energy in the desired direction rather than radiating it omnidirectionally. This characteristic can also be described by the antenna "beam width" which is determined from the radiation pattern of the antenna. For an isotropic antenna the radiation pattern would be in the form of a sphere, as shown in Fig. 4A, while the pattern of a typical circular parabolic microwave antenna would be in the form of a cone as shown in Fig. 4B. The angle θ of this cone at the 3 db. points is called the beam width, while the power gain of the antenna is proportional to the area of the sphere divided by the area of the cone for the same value of R. (Some energy is lost in side lobes not shown in Fig. 4B). Thus it is seen that the smaller the beam width, the higher the power gain.

Most antennas designed for microwave transmission can be readily analyzed through the use of simple optical principles. One such antenna, which is the electrical counterpart of the reflector in flashlights and automobile headlamps, is the parabolic antenna. Because of the simplicity of this antenna and its adaptability to a coaxial line feed, it is used in virtually all applications at, and below, 2000 megacycles.

Fig. 3A shows a parabolic curve, which from geometry, can be described by the following equation:

$$y^2 = 4Fx \quad . \quad . \quad . \quad . \quad . \quad . \quad . \quad . \quad (6)$$

where F, y, and x are as defined in Fig. 3A.

Two properties of the parabola make it particularly useful for focusing radiant energy. First, if a spherical wave source is placed at the focal point, any ray initiating from the focus is reflected in a direction parallel to the axis of the parabola; secondly, the distance traveled by any ray from the focus of the parabola to a plane x_1 at some distance away is always the same and is independent of the path taken. Therefore, as shown in Fig. 3A, a plane wavefront is transmitted with all points on the plane at the same phase.

Fig. 5. Doublet feed antenna system using disk reflector.

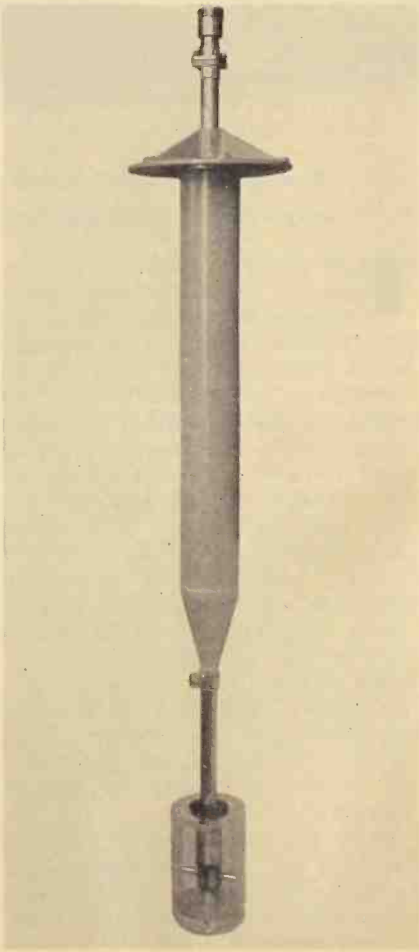

The parabola in Fig. 3A is represented only in the x-y plane. For most purposes the antenna is made parabolic in the z plane also and this antenna, shown in Fig. 2, is known as a circular parabola. For some applications, it is desirable to have a wide angle in the z plane and a narrow angle in the y plane (Fig. 4A defines the three planes with respect to earth) in which case the configuration shown in Fig. 6, known as a parabolic cylinder, can be used.

Conversion of the mathematical principle shown in Fig. 3A into a practical antenna involves a number of problems. For one, we have assumed a point source emitting spherical waves existing at the focal point. This can be effected by placing an isotropic antenna at this point. This type of antenna would illuminate the parabola properly but, however, it would also transmit energy outside the parabolic surface, which would either go into an undesired direction or be out of phase with the plane wave reflected from the parabola. This effect is called "spill over". The ideal characteristic of the focal point source would, therefore, be an antenna emittting a spherical wave over the parabolic portion only and be zero elsewhere.

In practice it is impossible to achieve such a pattern and some compromise between "spill-over" and uniform illumination must be effected. It has been noted empirically that best results are obtained with a feed which has a major radiation lobe striking the center of the reflector, its intensity decreasing smoothly to a value about 10 db. below maximum in the direction of the reflector boundaries and remaining small for all directions which do not strike the parabola. This pattern also allows for variations in space or geometric attenuation which occur in different parts of the wave front.

Another problem is physically attaining a point source which, of course, is a theoretical concept of an element which occupies no space. Since the feed antenna must have a finite length, its effect on the radiation pattern must be considered. It is obvious that the feed antenna will absorb a certain amount of energy at the center of the wave front. This introduces a "shadow" in the radiation pattern. This "shadow" can be minimized through use of an offset feed section as shown in Fig. 3B. This, however, decreases the gain and increases the magnitude of the minor lobes.

Another effect of having the feed antenna pick up some of the reflected energy is that a mismatch occurs in the feed line which is constant in amplitude but varies in phase as the frequency is varied. This mismatch can be compensated over a band by placing a raised plate at the apex of the reflector as indicated in Fig. 3C, but this plate also produces a harmful effect on the pattern. A trial and error procedure is usually employed to effect best results for a particular application. This is done by making a wooden model and spraying electrically important surfaces with metal. It is of course much easier to modify wood models.

The type of feed antenna used will depend upon the type of line used to connect transmitter to antenna. Generally, to match to a coaxial line a half wave doublet with a reflecting element is used. The reflecting element can be another doublet, a plane sheet, a half cylinder, or a disk. The disk, shown in Fig. 5, and the half cylinder appear to give best operation. It should be noted that a doublet does not have a spherical field and hence optimum polarization is not obtained. This factor limits the angle between focal point and rim of the reflector to a maximum of 140 degrees which is sufficient for most commercial applications.

Above 3000 megacycles it is practical to feed the parabola with the radiation from an open-ended wave guide. Where a circular parabola is used, a circular $TE_{1,1}$ wave guide should be used for a feed since it gives almost ideal phase and polarization characteristics. The aperture of this guide is

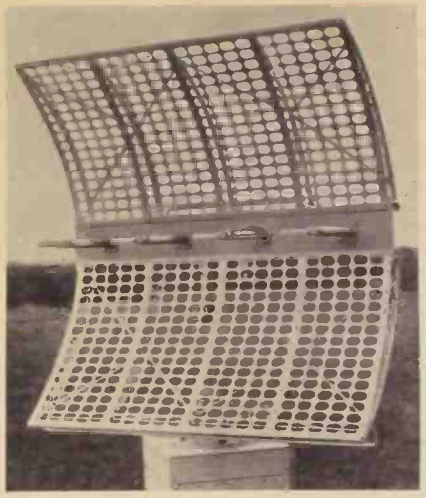

Fig. 6. Cylindrical parabolic antenna.

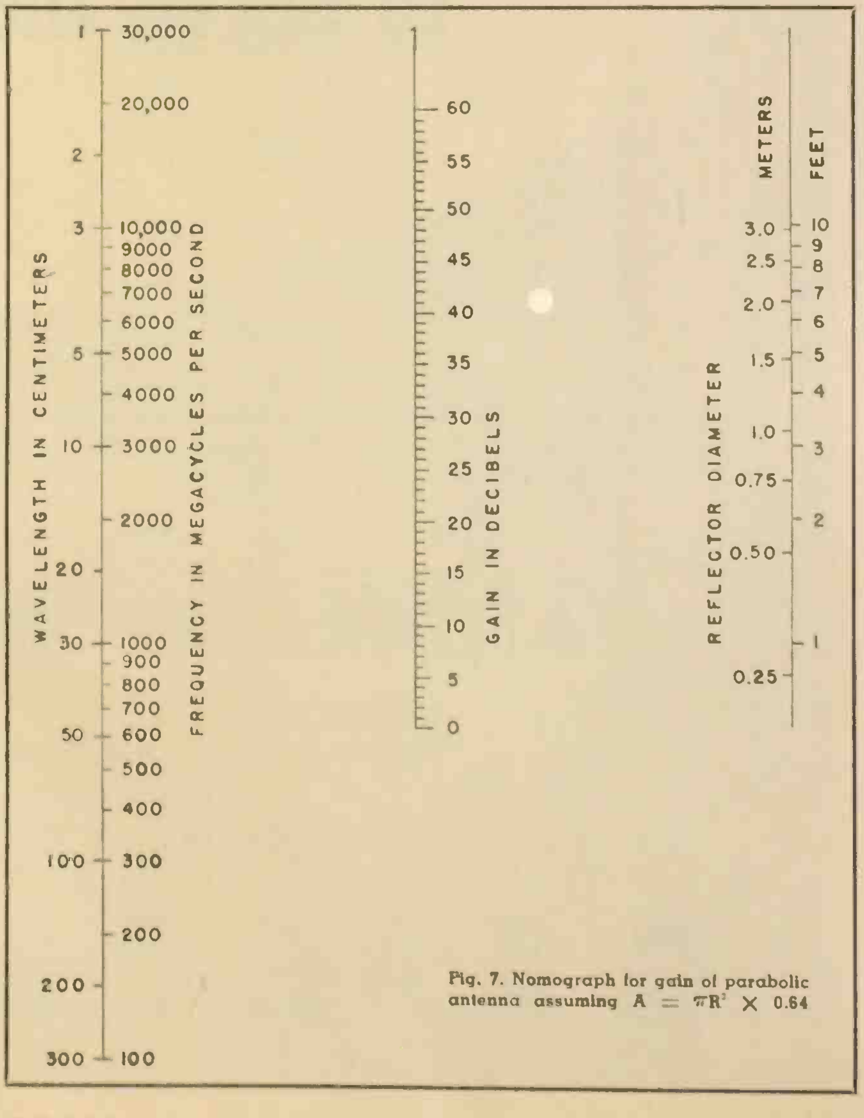

Fig. 7. Nomograph for gain of parabolic antenna assuming $A = \pi R^2 \times 0.64$

It is Our Privilege to serve the Leaders

THIS FREE BOOK — fully illustrated, with performance charts and application data — will help any radio engineer or electronics manufacturer to step up quality, while saving real money. Kindly address your request to Dept. 16.

ANTARA® PRODUCTS

GENERAL ANILINE & FILM CORPORATION

444 MADISON AVENUE
NEW YORK 22, N. Y.

G A & F® Carbonyl

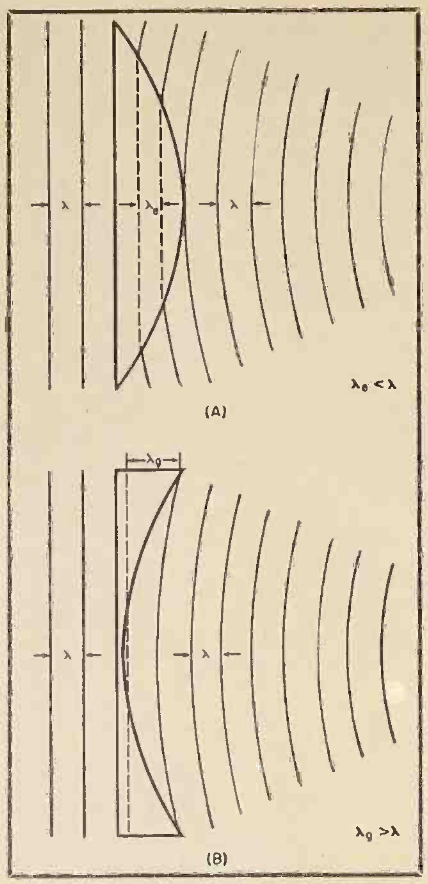

Fig. 8. Focusing action of (A) dielectric lens, and (B) metal type lens.

sometimes flared (increased in diameter in the shape of a horn) to improve directivity. Its dimensions are such as to support the dominant mode only.

A rectangular $TE_{1,0}$ wave guide does not generally give a circularly symmetrical radiation pattern, but is suitable for feeding a parabolic cylinder. The radiation pattern of a $TE_{1,0}$ feed is approximately elliptical so that the most efficient reflector area should be nearly elliptical, though for mechanical convenience it is more economical to use a rectangular shape.

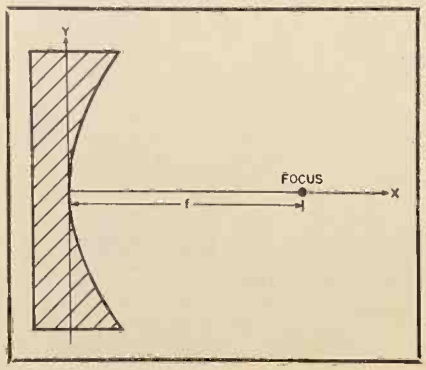

Fig. 11. Metal lens profile.

The effective area of the parabola is a function of the type of feed used and the shape of the reflector will therefore vary for different antennas. However, a close approximation of the effective area of most circular parabolas using either a doublet or waveguide feed is given by:

$$A = 0.64\,\pi R^2 \quad . \quad . \quad . \quad . \quad . \quad . \quad . \quad . \quad (7)$$

where R is the radius of the circle projecting across the parabola's rim.

The gain of this parabola, from equation (5), is equal to:

$$G = \frac{4\,\pi\,R^2 \times 0.64}{\lambda^2} \cong \frac{24.4R^2}{\lambda^2} \quad . \quad . \quad (8)$$

This equation is plotted on the nomograph shows in Fig. 7.

The beamwidth of the parabola is given by the equation:

$$\theta = \frac{70\lambda}{D} = \frac{35\lambda}{R}\,\text{degrees} \quad . \quad . \quad . \quad (9)$$

10-foot diameter parabolas are the maximum that are used for most commercial installations because of wind loading, tower rigidity requirements, etc. At 2000 mc. θ for a 10 foot dish is 3.7°.

As indicated previously, an open-ended wave guide excited at its input by a microwave generator will radiate energy into space. However, since the impedance of free space is different from that of the guide, a mismatch will exist at the guide termination and standing waves will be set up along the line. Furthermore, some of the energy will be diffracted at the opening of the guide causing the radiated energy to scatter and results in poor directivity.

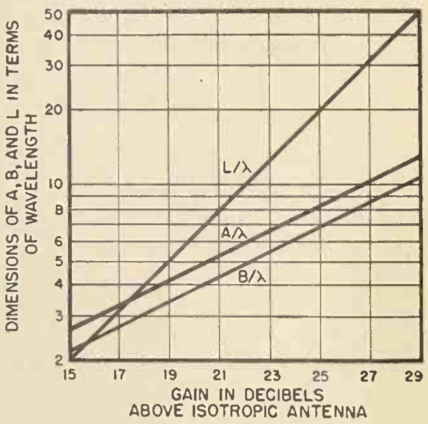

Fig. 10. Gain of electromagnetic horn.

To improve directivity and minimize mismatch, some type of transformer should be used between the guide and free space. The simplest type of transformer that would effect this result is a horn-shaped device, shown in Fig. 1, which operates in a similar manner to the exponential line described in a previous article[1]. The smaller the angle, β, (Fig. 1) is made, the more gradual the impedance transformation and the smaller the diffraction effect, so that the power gain is increased.

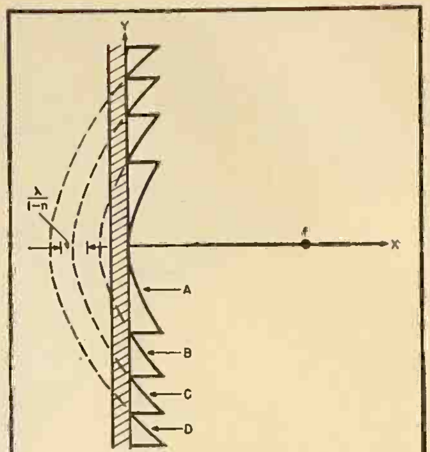

A—$(1-n^2)\ x^2-2f\ (1-n)\ x+y^2=0$

B—$(1-n^2)\left(x+\frac{\lambda}{1-n}\right)^2 -2\left(f+\frac{\lambda}{1-n}\right)(1-n)\left(x+\frac{\lambda}{1-n}\right) + y^2 = 0$

C—$(1-n^2)\left(x+\frac{2\lambda}{1-n}\right)^2 -2\left(f+\frac{2\lambda}{1-n}\right)(1-n)\left(x+\frac{2\lambda}{1-n}\right) + y^2 = 0$

D—etc.

Fig. 9. Profile of "step" metal lens.

It has been found that a definite relationship must exist between L, A, and B of Fig. 1 for optimum transmission. Fig. 10 plots these three parameters versus the gain in decibels. An approximation for the gain of an electromagnetic horn, for the case where $L > a^2/\lambda$, is given by the following equation:

$$G = \frac{10ab}{\lambda^2} \quad . \quad . \quad . \quad . \quad . \quad . \quad . \quad . \quad (10)$$

The beam width in the E plane is:

$$\theta_E = \frac{51\lambda}{b}\,\text{degrees} \quad . \quad . \quad . \quad . \quad (11)$$

while the beam width in the H plane is:

$$\theta_H = \frac{70\lambda}{ba}\,\text{degrees} \quad . \quad . \quad . \quad . \quad (12)$$

The effective area of the horn is a function primarily of its size. It is possible to calculate this effective area through the use of Eqt. (3) and the graph given in Fig. 10. A figure of 0.5(of $A \times B$) is frequently used as a typical value. (*Continued on page* 30A)

Fig. 12. Profile of path-length lens.

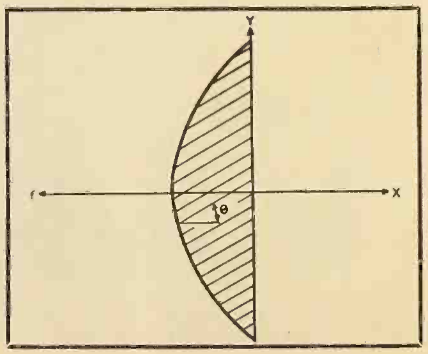

Performance PROTECTION

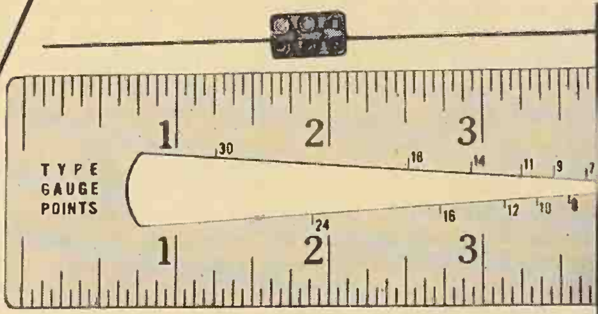

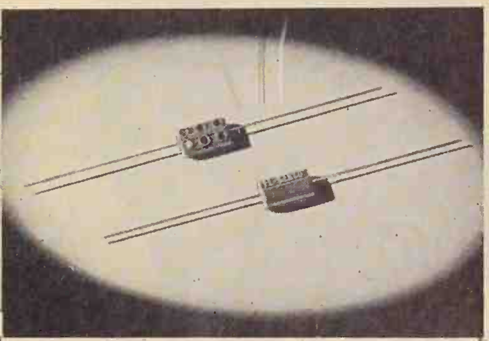

CM-15

Actual Size 9/32" x 1/2" x 3/16"
For Television, Radio and other Electronic Applications.
2 mmf. — 420 mmf. cap. at 500v DCw.
2 mmf. — 525 mmf. cap. at 300v DCw.
Temp. Co-efficient 50 parts per million per degree C for most capacity values.
6-dot Color Coded.

EL-MENCO CAPACITORS

Small, high-capacity fixed mica El-Menco capacitors are made to protect the performance of your products under severest operating conditions. They give long, dependable service because they must meet exacting conditions of Quality Test *before* they can be incorporated in your product. Tested at double their working voltage for dielectric strength, for insulation resistance and capacity value, El-Menco condensers can be depended upon for the utmost in performance protection.

SPECIFY EL-MENCO —

First Choice For Long Life and Dependability

THE ELECTRO MOTIVE MFG. CO., Inc.
WILLIMANTIC CONNECTICUT

Write on your firm letterhead for Catalog and Samples.

MOLDED MICA El-Menco MICA TRIMMER
CAPACITORS

FOREIGN RADIO AND ELECTRONIC MANUFACTURERS COMMUNICATE DIRECT WITH OUR EXPORT DEPT. AT WILLIMANTIC, CONN. FOR INFORMATION.

ARCO ELECTRONICS, INC. 135 Liberty St., New York, N. Y.—Sole Agent for Jobbers and Distributors in U.S. and Canada

Personals

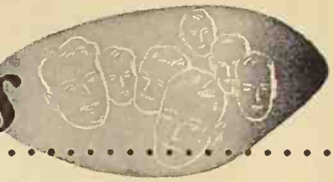

CECIL S. ALLEN has been named executive vice president and general manager of *Raytheon's Russell Electric Company* Division in Chicago. Prior to joining *Russell Electric*, Mr. Allen was vice president and general manager of the Pacific Coast Division of *A. O. Smith Corporation*, Milwaukee for two and one-half years. For sixteen years, Mr. Allen served in various capacities with *General Electric Company*.

C. J. BIVER has been appointed commercial engineer of the central region for *General Electric's* Tube Division, according to an announcement by E. F. Peterson, Manager of Sales for the division. Mr. Biver, whose headquarters will be located in Chicago, was application engineer for the Tube Divisions in the central region prior to his new appointment and was formerly commercial engineer for the *Ken-Rad Tube and Lamp Corp.*, at Owensboro, Ky.

JACK W. GARRISON, physicist at Armour Research Foundation of Illinois Institute of Technology, will head a newly organized nucleonics section in the physics department of the Foundation. Mr. Garrison joined the Foundation in 1948 after six years as research engineer for the *U. S. Gypsum Company*. He is a graduate of Butler University. This newly organized section at the Institute will apply radioactive tracer techniques to research problems.

DR. KENNETH H. KINGDON, formerly assistant director of the *General Electric* Research Laboratory at Schenectady, has been appointed technical manager of the Knolls Atomic Power Laboratory. Dr. Kingdon, who was one of the first scientists to isolate appreciable quantities of the energy-releasing form of uranium U-235 from the natural element, has been with the Research Laboratory since 1930, and has headed its atomic power work since 1946.

KEN RANDALL, former associate of *M. J. Shapp Company*, will take over representation of the *Barry Corporation, Condenser Products Co., Electric Motor Corp., Cyclohm Motor Corp., Thordarson Electric Mfg. Co., The Workshop Associates, Inc.*, and *Switchcraft, Inc.* Mr. Randall has been associated with *Sears, Roebuck* and *RCA* in various capacities. Milton J. Shapp will devote his full time as President of the *Jerrold Electronics Corporation* of Philadelphia, Pa.

DR. GEORGE W. VINAL, Chief of the Electrochemistry Section of the National Bureau of Standards, has retired after more than forty-two years of distinguished service to the Government. Best known for his classical book, Storage Batteries, Dr. Vinal has contributed extensively to scientific journals and is internationally known for his research in the field of electrochemistry and the development of the silver voltammeter and the standard cell.

These Leaders look to SYLVANIA for dependable TV Picture Tubes

Admiral

air-king

Arvin

Bendix Television

Calbest

CONRAC

CROSLEY

DEWALD

Emerson Television

FADA

hallicrafters

Hoffman

INDUSTRIAL TELEVISION INC.

Kaye-Halbert

Magnavox

Meck

MIDWEST

Motorola

national

Olympic

Packard Bell

phaostron

PHILCO

PILOT

SCOTT

Sentinel

Silvertone

Sparton

Starrett

STROMBERG-CARLSON

SYLVANIA

Tele King

Tele-tone

TRAV-LER

Westinghouse

• The trade-marks shown here identify the television leaders now choosing and using Sylvania TV Picture Tubes in their sets.

The reasons behind today's acceptance of Sylvania tubes include greater clarity, consistent color, dependability, and longer life.

Remember, your dealers as well as set owners recognize Sylvania as a symbol of distinction—a name associated with the very finest in radio and television.

For full descriptions and ratings of all Sylvania TV Picture Tubes, write today to Sylvania Electric Products Inc., Dept. R-2310, Emporium, Pa.

SYLVANIA ELECTRIC

RADIO TUBES; TELEVISION PICTURE TUBES; ELECTRONIC PRODUCTS; ELECTRONIC TEST EQUIPMENT; FLUORESCENT TUBES, FIXTURES, SIGN TUBING, WIRING DEVICES; LIGHT BULBS; PHOTOLAMPS; TELEVISION SETS

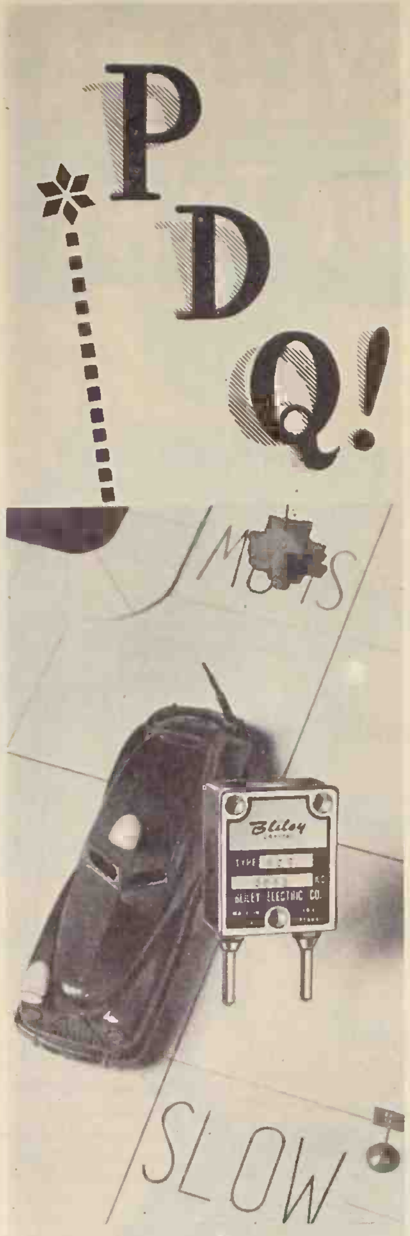

NEWS BRIEFS

OVEN LOADING TECHNIQUE

Jesse Sherwood of the National Bureau of Standards has developed a new oven loading technique for use in the atomic-beam clock program to overcome the problem of the introduction of highly reactive materials, such as alkali metals, into the oven which acts as the beam source.

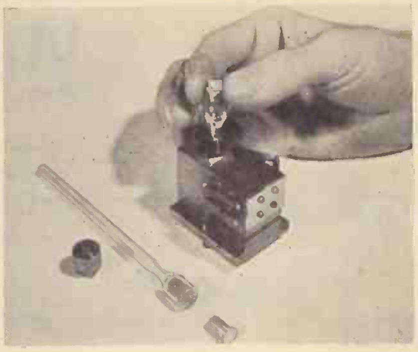

In the new technique, the oven used with the atomic-beam magnetic resonance apparatus is of a conventional type, but the cesium metal is distilled into a specially designed ampoule and sealed off under vacuum. The ampoule contains a well into which is inserted a carefully lapped aluminum plug of about 7 mm. diameter. This plug is removed before filling and then set firmly in place after sealing. When the ampoule is heated to 80-100° C, it will crack because of the larger thermal expansivity of aluminum, referred to glass.

With this new method, it is possible to load the oven, carry out further checks on the experimental conditions, and pump out the system before exposing the active metal.

ELECTRONIC TRAFFIC SYSTEM

The city of Denver, Colorado, has launched a $125,000 modernization plan of its entire downtown network of traffic signals and controllers which will employ a revolutionary combination of fixed-time-cycle and electronic traffic control equipment.

Initially, the installation will include 104 *General Electric* type F traffic controllers to be supervised electronically by a master cycle selector. All controller dial units and the master selector will be remotely housed on a central control panel in Denver's City and County building, and individually connected to the controller switching mechanisms in control boxes at 104 downtown intersections.

In this new system any cycle timing between 40 and 125 seconds as well as red-green light percentages will be electronically adjusted. Every six minutes the electronic master selector will add up this traffic count, compute the proper timing cycle and red-green splits to handle the traffic flow, and then automatically adjust the individual controllers by varying the voltage and frequency on their synchronous drive motor.

NEW GAUGE MEASURES "NOTHING"

Scientists at the *Westinghouse Research Laboratories*, Pittsburgh, Pa., have revealed a new instrument called an "ion gauge" which can detect the presence of air in a vacuum where only one air molecule remains out of every 10,000 billion originally present.

This supersensitive gauge looks like a large radio tube and behaves in a similar manner. The gauge was developed by Robert T. Bayard, under the supervision of Dr. Daniel Alpert, head of the inter-atomic physics section. Dr. Alpert explained that for measuring ordinary low pressures, scientists use a column of mercury whose height corresponds to the atmospheric pressure which is about 30 inches. Using the new gauge, pressures that would raise a column of mercury only one-thousandth of a billionth of

(*Continued on page* 29A)

Oscillograph Amp.

(*Continued from page 7A*)

ing, no special precautions were taken in the circuit to minimize drift. A regulated heater voltage can be used if desired. A lead from the heater transformer provides a convenient source of calibrating voltage. The input leads are shielded cable and are connected to the amplifier through coaxial-type relays, which maintain the integrity of the shielding, and make possible the convenient connection or disconnection of the input. Small gaps provide protection against accidental overvoltages. The plate circuit requires 0.5 ampere at 125 volts direct current. A small motor-generator set is the most convenient source of plate voltage, since it is independent of line-voltage fluctuations and can carry a number of amplifiers without overload.

Preparatory to operation, the amplifier is balanced and the gain adjusted for a satisfactory oscillograph deflection. With the balance meter (see Fig. 1A) in the circuit, the variable resistor in the cathode circuit of the first stage is adjusted to give a zero reading. Then, with the oscillograph in the circuit, the input-voltage dividers are adjusted to give the required deflection.

This amplifier, with its double-input feature, is particularly useful in line-dropping tests, in which the voltage across the terminals of a circuit breaker is to be measured. For example, in the circuit of Fig. 1B, the voltage across the breaker on opening is required. The double input permits the voltage across the two capacitance dividers to be measured with the amplifier, power supply, and oscillograph grounded. If a single-input amplifier were used, all apparatus would have to be insulated from ground, which is inconvenient and can lead to measurement errors.

The relays on the amplifier chassis are a convenience in tests of this type. By opening the circuit to one divider the gain can be adjusted for proper deflection. Furthermore, the relays make possible rapid disconnection of the amplifier if draining of the voltage divider must be avoided.

The measuring circuits ahead of the amplifier must be arranged so that the signal appearing at the amplifier input is faithful to the original voltage. These circuits will depend on the particular measurement required, and are a separate problem in themselves.

Although the amplifier is not on the market, it consists of standard components available from radio parts suppliers, and can be assembled by any competent meter shop. The cost is so small that practically any job that can use such a device warrants its construction.

NEW PRODUCTS

TV POWER SUPPLIES

General Electric Company, Syracuse, N. Y., has announced two new regulated power supplies for television station applications. Both units, types TP-12-A and TP-13-A, feature single-phase input, high current capabilities and low ripple.

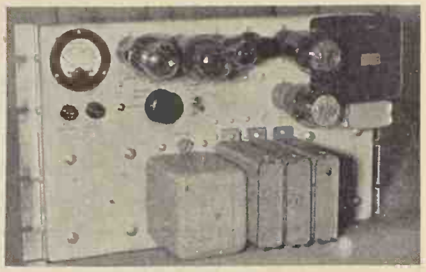

The TP-12-A can supply 300 to 900 milliamperes at 275 to 300 volts with a maximum ripple of less than 0.01 volts peak-to-peak. The TP-13-A can supply 0 to 300 milliamperes at 275 to 400 volts with a maximum ripple of less than 0.05 volts peak-to-peak.

Further information on these power supplies is available from the *GE* Commercial Equipment Division at Electronics Park, Syracuse, N. Y.

LABORATORY MONITOR

Model 1615 Radiation Sentinel laboratory monitor for alpha-beta-gamma detection announced by *Nuclear Instrument and Chemical Corp.*, 229 West Erie St., Chicago 10, Ill., may be used for checking clothing, benches, glassware, and hands or fingertips for contamination, or for continuous monitoring of background air contamination or isotope decay.

This model may also be used to count samples with activities between 100 and 50,000 counts per minute where accuracy of measurement need not be better than 3% standard error. A choice of five different ranges, from 500 to 50,000 counts per minute full scale, is provided. A chart recorder may be attached for maintaining a permanent written record.

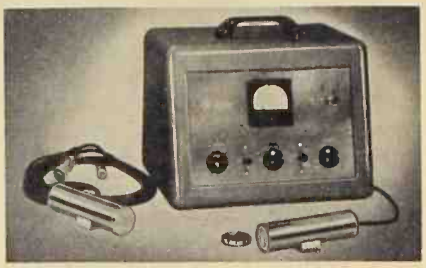

FREQUENCY METER

Now available from *Gertsch Products, Inc.*, Los Angeles 25, California, is its new FM-1 v.h.f. frequency meter which reads the frequencies direct. The range is from 20 to 480 mc.

It is guaranteed to be accurate to within .005% in the temperature range of 32° to 120° F., and operates from dry batteries or from a regulated laboratory power supply. Provision is made to modulate the carrier approximately 30% at 1000 cycles.

2000-MPH TIMING EQUIPMENT

The Temporal Sequence system announced by *Beckman & Whitley, Inc.*, 914 San Carlos Ave., San Carlos, California, is based on slit-type camera techniques which can record and measure velocity and acceleration of objects moving at 2000 m.p.h. in a single optical image.

To measure optical events, a slit camera records time sequence past or within a vertical plane passing through the optical axis of the lens. Besides photographing the event, this equipment automatically records, on the same film, electronically-timed numbers showing elapsed seconds and hundredths with intermediate pips spaced at thousandths of a second.

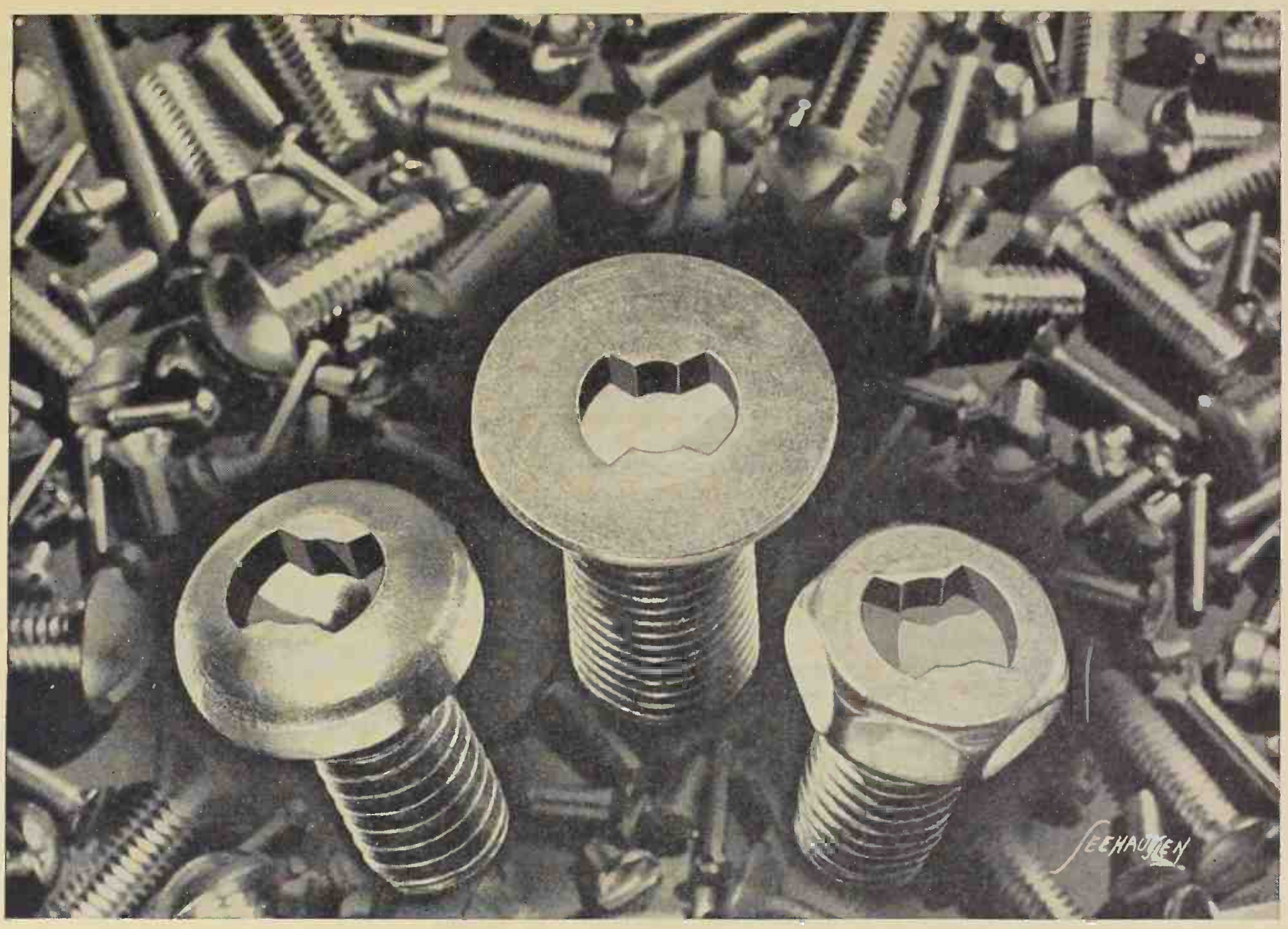

TYPE "A" ASSEMBLY BIT

CLUTCH HEAD *Invites Comparison With* ALL *Other Screws...*

. . . RECESSED HEADS AS WELL AS SLOTTED

It is generally conceded that recessed head screws have outmoded the use of slotted head screws on modern assembly lines. For that reason, CLUTCH HEAD user quotations . . . recording production increases ranging from 15% to 50% . . . are based on comparison with *other types of recessed head screws.*

Only Clutch Head provides Center-Pivot entry for safe automatic straight driving.
Only Clutch Head has non-tapered driving to eliminate the skid hazard of "ride-out."
Only Clutch Head offers this all-square driving contact as a safety factor.
Only Clutch Head eliminates the fatigue of end pressure for easier, faster driving.
Only Clutch Head has the Lock-On which permits one-handed driving from any angle.
Only Clutch Head delivers Bit durability that drives up to 214,000 screws, non-stop.
Only Clutch Head has a recess basically designed for common screwdriver operation.

COMMON SCREWDRIVER

America's Most Modern Screw invites you to make your own comparison . . . to evaluate these exclusive CLUTCH HEAD features...right at your own desk. Your request will bring you, by mail, package assortment of screws, sample Type "A" Bit, and Illustrated Brochure.

CLUTCH HEAD SCREWS

UNITED SCREW AND BOLT CORPORATION

CLEVELAND 2 CHICAGO 8 NEW YORK 7

Work-Coils

(*Continued from page* 6A)

a straight conductor parallel to a plate of conducting material. A sectional view of this arrangement is shown in Fig. 9, where the radius of the cylindrical conductor is *a* with its center at a distance *h* away from the conducting plate.

Considering the *X* and *Y* axes in the plane of the figure and the *Z* axis perpendicular to the plane of the figure, the numerical values of (16) and (17) are zero while that of (18) becomes

$$H_z = \frac{I\sqrt{1-(a/h)^2}}{\pi h[1-(a/h)^2+(y/h)^2]} \quad (19)$$

The series of graphs of Eqt. (19) shown in Fig. 11 indicate the distribution of H_z on a conducting surface for different values of the ratio a/h.

With the aid of Eqts. (10) and (11) the formulas for P_w and for P_c are calculated for the metallic load and the current carrying conductor.

The ratio of P_w/P_c then provides a simple means for obtaining the coupling efficiency for this arrangement. This efficiency as expressed by Eqt. (12) is:

$$\eta = \frac{1}{1+\frac{h}{a}\left[\frac{\mu_c\sigma_w}{\mu_w\sigma_c}\right]^{1/2}} \quad . \quad . \quad . \quad . \quad . \quad (20)$$

and is illustrated in Fig. 13 for different conductor spacings. Although these results are based upon a single cylindrical conductor in the vicinity of a metallic sheet as a load, they are very indicative of expected results for more complicated arrangements. When the conductor and the metallic sheet are made of the same material, the quantity under the radical sign in Eqt. (20) is unity, and the maximum coupling efficiency will exist when the ratio h/a is also unity. Since the ratio h/a cannot be less than unity and may increase to any value, the graph in Fig. 13 has been plotted with the ratio a/h as the abscissa. All physically possible values for a/h lie between zero and unity and provide a condensed coordinate system.

Fig. 17. Current concentrator arrangement for soldering or braying four joints simultaneously.

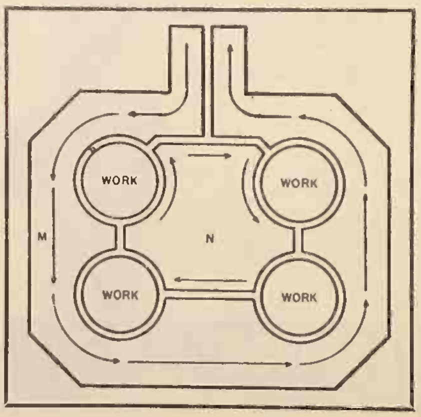

The operation and performance of a single conductor in the vicinity of a conducting sheet has been presented by Eqts. (19) and (20) and Figs. 9, 11, and 13. These formulas and graphs are of value as they are, but in order to have a more complete point-of-view of this subject, similar but supplementary formulas should be included for two and three conductors. This becomes more evident when it is realized that two and three turn work-coils are frequently used in conjunction with current transformers. To modify the formulas of a single conductor arrangement, consider the conductor location in Figs. 14A and B. By noting that there are two conductors in Fig. 14A and three in Fig. 14B, and applying Eqt. (19), with *a* equal to zero, to each conductor, the current distribution in the load is plotted in Figs. 15 and 12. It is quite obvious that the current distribution in the load is not flat for one, two or three conductors but peaked and therefore will give temperature striations when very short heating cycles are used. This effect becomes less pronounced for smaller values of the ratio a/h.

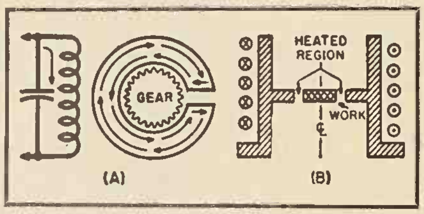

Fig. 16. (A) Basic schematic arrangement of induced-current concentrator. (B) Arrangement of current concentrator and work.

In order to illustrate the practical application of Eqts. (16), (17), and (18), consider a work-coil satisfying the plane-curve of a Spiral of Archimedes. This coil will lie in a plane and will produce an axial magnetic field. If we consider the coil to lie in the *x-y* plane with the origin of the coordinate system coinciding with the center of the coil, the magnetic intensity produced by this coil will lie entirely along the *z*-axis.

By applying Eqts. (16), (17), and (18) to the current carrying coil in the shape of this spiral, a set of equations is obtained in terms of the rectangular coordinate system. Since it is much more convenient to express these equations for the spiral in terms of polar coordinates, let (r, θ) be the polar coordinates of a point (X, Y) on the two dimensional spiral. The general form of the polar equation is :

$$r = f\ (\theta) \quad . \quad . \quad . \quad . \quad . \quad . \quad . \quad . \quad (21)$$

where θ is the curve parameter. The transforming equations which transform from the rectangular system to the polar system of coordinates, when substituted in Eqt. (9), yield equations in the form of (16), (17), and (18). In this particular application, H_X and H_Y are zero while the magnetic field intensity along the *Z*-axis is:

$$H_z = \int_{\theta_0}^{\theta_1} \frac{d\theta}{f(\theta)} \quad . \quad . \quad . \quad . \quad . \quad (22)$$

For the spiral under consideration, the evaluation of Eqt. (22) is direct and yields:

$$H_z = 2\pi n\ log_e\ r_1/r_0 \quad . \quad . \quad . \quad . \quad . \quad (23)$$

Since the power delivered to a load varies as the square of H_z, for the spiral type of coil, it is quite evident that it is necessary to make the number of turns *n* as large as size permits and V_o as small as possible. A coil of this type but with a curved surface is very well exemplified in Fig. 3 and provides a work-coil with a very strong magnetic field in the direction parallel to its axis.

In order to concentrate the induced currents to the desired regions of heat treating, Babat and Losinsky have developed the concept of the *eddy-current concentrator*. Their basic idea is to arrange the work-coil in such a manner that its surface is type zero from a topological standpoint. Schematically we may refer to the diagram in Fig. 16A which shows the path of the tank, work-coil and work-currents with the aid of arrows. A sectional drawing of the primary coil and special work-coil concentrator is shown in Fig. 16B with the heated regions indicated. Although the same fundamental laws of design of work-coils apply to the current-concentrator type, under certain kinds of loads, this type accomplishes its purpose with greater ease.

Another example of the current-concentrator principle is that shown in Fig. 17, where four lugs are being brazed to a cap by means of a single-turn coil. The outer portion of the work-coil is identified by the letter *M* and carries the work-coil current. The concentrator, which is cut to fit around the lugs, is marked *N*.

Thus we have seen, from the foregoing discussion, that the design of work-coils for induction heating is best accomplished by combining the mathematical approach with that of the experimental. Either method alone is quite unsatisfactory and time consuming. It is important to realize this when designing work-coils and by carefully applying the theory and selecting critical coil parameters, the final design may be achieved in a few experimental steps.

The author desires to express his appreciation to the *Induction Heating Corporation* for the accompanying work-coil photographs.

TECHNICAL BOOKS

"DISSOCIATION ENERGIES" by A. G. Gaydon, D.Sc. (London). Published by *Dover Publications, Inc.*, 1780 Broadway, New York 19, N. Y. 239 pages. $3.95.

In this clearly written and illustrated text Dr. Gaydon has attempted to clarify the inconsistencies and unsolved problems which exist in present literature on dissociation energies. The results of recent research in the field are here recorded and analyzed, and the author has included a discussion of part of the theory of molecular spectroscopy because of the importance of accurate determination of the values of the dissociation energies of diatomic molecules.

There are chapters on the determination of dissociation energies by thermal methods and by controlled electron impact, although the approach is chiefly from a spectroscopic standpoint. Numerical data for about 250 diatomic molecules, together with the values which the author believes are most likely to be correct, are also included in this book.

"ELECTROMAGNETIC THEORY" by Oliver Heaviside. Published by *Dover Publications, Inc.*, 1780 Broadway, New York 19, N. Y. 386 pages. $7.50.

To celebrate the centennial anniversary of Oliver Heaviside's birth, *Dover Publications, Inc.*, has published this new edition of his well-known, unconventional examination of nineteenth century electrophysics.

This interesting book is an unabridged edition of volumes 1, 2, and 3 which were originally published between 1891 and 1912. Everything relating to electrical induction—the energy of electric currents, the forces and fluxes of energy in the electromagnetic field, etc.—has been worked out by the author in careful detail. Subjects include Maxwell's theory, eolotropic relations, the electrostatic stress in air, Lagrange's equations, scientific limitations on human knowledge, and over 500 other topics.

Although the author offers no up-to-the-minute treatise on communication theory, nuclear fission or electronics, readers will find that Heaviside's genius for instilling into his writings the flavor of his own personality makes this book one of the most popular and readable works in applied science.

A critical and historical introduction by Ernst Weber, Director, Microwave Research Institute, Polytechnic Institute of Brooklyn was prepared especially for this edition.

* * *

News Briefs

(*Continued from page* 24A)

an inch can be detected and measured.

Although the gauge was developed specifically to aid Dr. Alpert in the study of the behavior of atoms, electronics, and radiation in gas-filled tubes, it is expected that the instrument will find widespread use in other fields.

PRODUCTION OF TEFLON

A new unit of the *Du Pont Company's* plastics plant near Parkersburg, W. Va., has gone into commercial production of Teflon tetrafluoroethylene resin. This unit makes available to the chemical and electrical industries and other users of Teflon a productive capacity several times that of the plant at Arlington, N. J., where manufacture of the material in relatively small commercial quantities was started in 1943. This completes the first expansion started at the Parksburg plant less than two years ago with the commercial manufacture of nylon molding powder, tapered bristles, etc.

For the next few months the unit will produce granular Teflon only. Further expansion is under way for the manufacture of the new Teflon Suspensoid.

* * *

Fluorescence

(*Continued from page* 10A)

sub-assemblies are by plug and socket or, in the case of the swiveling knuckle joint, by slip rings. Power is supplied by two size D flashlight dry cells which give an operating life of about 12 hours on a 50 per-cent duty cycle.

For the ultraviolet examination of large areas, where light levels are reasonably low, the dark-chamber is removed and the handle with generator and filter unit attached, can be used as a wand in the manner of an ultraviolet "flashlight". This method is useful in checking for rodent or insect infestations in food warehouses, identification of persons marked with fluorescent tracing powders, and such techniques.

A circuit of the unit is provided in Fig. 3. A modified 2-volt vibrator interrupter is driven by the dry cells through a series resistor which limits current. Approximately 2.9 volts is developed across each half of the primary winding. The turns ratio of the power transformer is such as to supply 350 volts r.m.s. across the terminals of the light source. This is a specially-made low-pressure cold-cathode mercury-vapor discharge tube wound in a flat spiral with approximately 1¼ in. outside diameter. Corning Vycor brand glass is used. This lamp produces 93 per cent of its output in the spectral band at 2537 Angstroms. No radiation is emitted below 2000 A., thus no ozone is produced to interfere with passage of ultraviolet or cause other possible undesirable effects.

Fig. 3. Circuit of Fluoretor

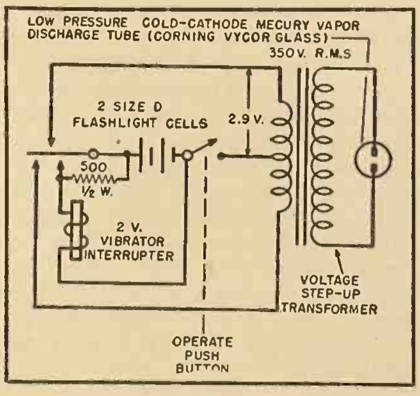

* * *

Microwave Antennas

(*Continued from page* 20A)

The horn, which is similar in many respects to the acoustical horn, finds its widest application as a feed for either a parabolic or lens antenna at frequencies where wave-guide transmission lines are used.

Lens Antennas

Another optical device that can function as an antenna is the lens, which performs in a manner similar to that of the parabolic reflector in that it transforms a spherical wave into a uniphase wave at the aperture of the lens.

As in the case of the optical lens, the focusing action depends upon a change in phase velocity of the spherical wave as it goes from one medium to another. The lens may take two forms; the dielectric type, shown in Fig. 8A, in which the velocity of the wave is decreased by the medium or dielectric, or the metal type, shown in Fig. 8B, in which the phase velocity is increased in the medium, the medium being comprised of a series of parallel plates.

It can be shown that when a electromagnetic wave is confined between conducting plates which are parallel to the electric vector and spaced apart a distance greater than one half wavelength, its phase velocity is greater than its free space velocity. When the plates are separated by air, the effective index of refraction is equal to[6]:

$$N=\sqrt{1-\left(\frac{\lambda}{2a}\right)^{2}}\ ,a>\frac{\lambda}{2}\quad . \quad . \quad (13)$$

where a is the spacing between the conducting plates.

The profile of a metal lens is shown in Fig. 11. The curvature of this lens can be determined from the following equation:

$$(1-N^2)\,x^2-2\,(1-N)\,fx+y^2=0\quad . \quad . \quad (14)$$

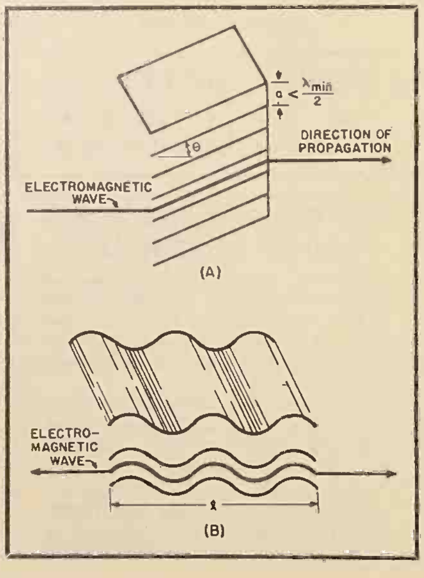

Fig. 15. Dielectric effect achieved by (A) slanting plates and (B) serpentine plates.

This is the equation of an ellipse having a radius of curvature, at $y=0$, of:

$$r=f(1-N)\quad . \quad . \quad . \quad . \quad . \quad . \quad . \quad (15)$$

A lens of this type would have considerable thickness at the top and bottom. It is possible to reduce this thickness through the use of a system of steps, shown in Fig. 13, in which the thickness of each step is equal to:

$$t=\frac{\lambda}{1-N}\quad . \quad . \quad . \quad . \quad . \quad . \quad . \quad (16)$$

Fig. 9 shows the equations of the curves for the successive steps.

The dielectric type of lens can be obtained by using slanted or serpentine conductors, as shown in Fig. 15, so that it will take the waves a longer period of time to traverse the distance involved because of the longer path taken. The index of refraction for this type of lens is equal to[8]:

$$N=\frac{1}{\cos\theta}\ \text{for slanted type}\quad . \quad . \quad (17)$$

$$N=\frac{l}{l_o}\ \text{for serpentine type}\quad . \quad . \quad (18)$$

and the equation of the curve shown in Fig. 12A is:

$$(N^2-1)\,x^2+2fx\,(N-1)-y^2=0\quad . \quad . \quad (19)$$

This lens has the advantage over the previously described metallic lens in that it provides broader bandwidth, greater simplicity, and less severe tolerances.

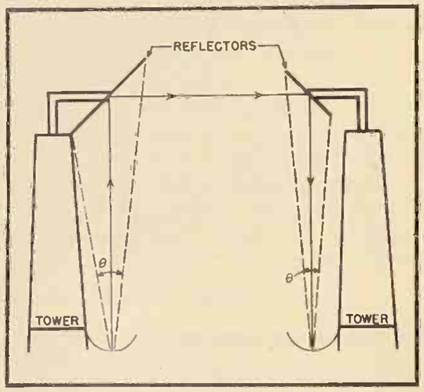

Fig. 14. System of reflectors used to minimize transmission line losses.

Use of Antennas as Transmission Lines

For installations where long lengths of transmission line are required to reach the antenna, a serious problem of excessive attenuation and expense is involved. For these cases a system of reflectors, shown in Fig. 14, in which the antenna is placed on the ground and beamed toward a reflector which in turn directs the wave in the desired direction, can be employed. Usually the antenna beam is perpendicular to the ground, and the reflector is at a 45 degree angle.

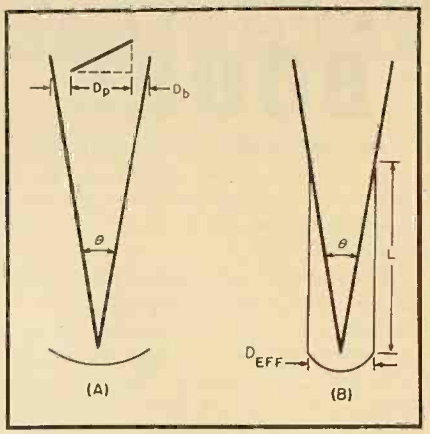

Fig. 13. Parameters for calculating the power reflected from a reflector.

Simple geometry can be used to determine the per-cent of power that is reflected by the reflector. The reflected power is equal to the ratio between the projected area of the reflector divided by the area of the beam at the reflector point. Referring to Fig. 13A, the power reflected becomes:

$$P_r=\left(\frac{D_b}{D_p}\right)^2\quad . \quad . \quad . \quad . \quad . \quad . \quad (20)$$

where D_p and D_b are the diameters of the projected reflector and the beam respectively. It should be noted, of course, that P_r cannot be greater than 1, hence Eqt. (20) holds only for $D_p<D_b$.

Another factor that should be remembered is that the antenna does not act as a point source but generates a wave of finite length equal to the effective area of the antenna. This area projects in the direction of the major lobe until the projected line crosses the theoretical beam line as shown in Fig. 13B.

The length, L, in this figure is, from geometry, equal to:

$$L\theta=D_{eff};\ L=\frac{D_{eff}}{\theta}\quad . \quad . \quad . \quad . \quad (21)$$

with θ, the beamwidth, in radians.

For a parabolic antenna with an effective area of 0.64, or an effective diameter of 0.8, Eqt. (21), using the value of θ given in Eqt. (9) converted to radians, becomes:

$$L=\frac{0.8D}{\theta}=\frac{0.8D}{\frac{70}{57.3}\cdot\frac{\lambda}{D}}=\frac{D^2}{1.5\,\lambda}\quad (22)$$

A very recent development in the transmission line art that shows great promise for the future is the surface

Fig. 16. Schematic sketch of a surface wave transmission line.

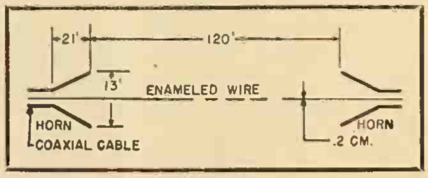

ave transmission line. This line, also own as the G-String and G-Line, is ll in the experimental stage but pubhed results[10] indicate a very great provement in attenuation can be hieved. For example, for the 120 foot e shown in Fig. 16, the measured attnuation was 2.2 db. at 1600 mc.; 2.3 . at 3300 mc.; and 4.5 db. at 4500 mc. is compares very favorably with an uivalent length of RG-8/U cable ich has an attenuation of 13 db. at 00 mc.; 22 db. at 3300 db.; and 30 db. 4500 mc.

This line utilizes an entirely new inciple in microwave transmission le design in that the electromagnetic ergy is not transmitted via a guided diated wave, but is confined within the rface of the transmission line. It can shown that if a TEM wave can be nerated with a z component, it will t radiate into space, but will be coned within the surface of the wire.

The author is grateful to Mr. A. G. avier, *Federal Telecommunication bs.*, for his permission to use his rmograph of parabolic antenna gain.

BLIOGRAPHY:

. *Racker, J., "Microwave Receivers"*, RADIO-CTRONIC ENGINEERING, *July, August*, 1950.
Racker, J., "Microwave Transmitters", RA-ELECTRONIC ENGINEERING, *May, June*, 1950.
Racker, J., "Microwave Techniques", RA--ELECTRONIC ENGINEERING, *Feb.*, 1950.
. *Racker, J., "Microwave Transmission es"*, RADIO-ELECTRONIC ENGINEERING, *March*, 0.
Racker, J., "Microwave Components", RA-ELECTRONIC ENGINEERING, *April*, 1950.
Kock, W. E., "Metal Lens Antennas", IRE, ., 1946.
Kock, W. E., "Path Length Microwave ses", IRE, Aug., 1949.
. *Friis & Lewis, "Radar Antennas", Bell tem Technical Journal, April*, 1947.
Cutler, C. C., "Parabolic Antenna Design Microwaves", IRE, Nov., 1947.
0. *Goubau, G., "Surface Wave Transmission e"*, RADIO-ELECTRONIC ENGINEERING, *May*, 0.

The following information is published in order to clarify a misunderstanding created by the publication of Dr. Georg Goubau's talk n "Surface Wave Transmission Line" in the May 1950 issue of his magazine.

It should have been indicated hat this material was the trancript of a talk given by Dr. Goubau t the Annual IRE Convention in New York City on March 8, 1950 nd not a special article written by im for this magazine.

PHOTO CREDITS

ages	Credit
A, 4A, 5A	Induction Heating Corp.
A	Westinghouse Elec. Corp.
A, 9A	Philco Corp.
0A	Menlo Research Lab.
1A, 12A, 13A	Northwest Airlines, Inc.
5A, 17A	Bell Telephone Labs.
6A	Federal Telecomm. Labs.

Radio Navigation

(*Continued from page* 14A)

reaches zero for then the output of the phase sensitive amplifier will be zero. It follows that the card will indicate phase angle and therefore bearing, hence the name Omni-Bearing Indicator.

Fig. 2 shows a simplified form of a resolver circuit. The grids of the tubes are fed 30 cycle signals 90 degrees displaced from each other. The resolver or phase shifter stator coils, being in series with the comparatively large resistors in the cathode circuits, carry constant currents. By virtue of the construction of these coils coupled with the fact that they are fed out of phase currents, they produce a rotating field. For each mechanical degree through which the resolver is turned there will be a phase displacement of 1° in the induced rotor voltage.

The 30 cycle signal developed in the discriminator as described previously is fed to a phase splitting network ahead of V_{203} and V_{202} as shown in Fig. 9. The purpose of this network is to supply the four grids with voltages 90 degrees separated from each other. The two resolvers shown symbolize the ones in the pilot's Omni-Bearing Selector and in the Omni-Bearing Indicator in the accessory unit.

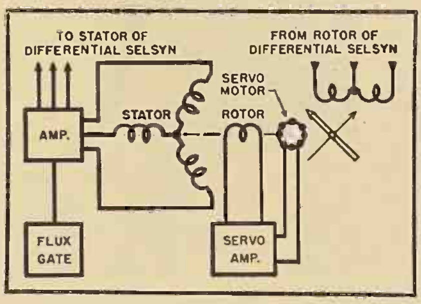

Fig. 10. Automatic circuits. Differential selsyn is shown in Fig. 6.

From the output of the auto resolver the reference signal, after some further mistreatment, arrives at the primary of T_{205} whose secondary appears in Fig. 8. Our variable signal shows up in the primary of T_{204}. Operation of the deviation indicator from these two secondaries can easily be deduced from observation of Fig. 8.

Three phase voltage containing direction information from the flux gate (gyrosyn compass) appears in the stator of the RMI card drive motor as shown in Fig. 10. Direction information is contained in the amplitude relationship of the three phases. Voltage induced in the rotor is amplified in a servo amplifier whose output drives a servo motor on the same shaft and this positions the rotor to null with the stator. The compass card on this shaft then reads magnetic heading.

With GCA (Ground Control Approach) and Teleran already accepted, and other developments rapidly coming to the fore, it appears that full automatic flight control is no longer just a dream of the future.

REFERENCES

Busiganies, H.: "High-Stability Radio Distance-Measuring Equipment for Aerial Navigation," Electrical Communication, p. 237, *Sept.* 1948.
"Visual-Aural Ranges and Omniranges," Bulle-Aeronautics Administration.
"Distance Measuring Equipment and Offset Course Computer," Bulletin No. 4, U. S. Dept. of Com., C.A.A.
Gross, Francis J. and Kay, Hugh: "Flight Tests of an Off-Schedule Distance Computer, Technical Development Report No. 93, *C.A.A.*
Schuck, O. H.: "Computer for Aeronautical Navigation," Proceedings of the National Electronics Conference, Vol. 3, 1947.

ENGINEERING DEPT.

OFF-RESONANCE RESPONSE—LARGE DEVIATION

CHESTER W. YOUNG, Senior Electronic Eng., Consolidated Vultee Aircraft Corp.

THIS nomograph is an aid in finding the response of a circuit to a given frequency which is greater than 3/Q times the resonant frequency of the tuned circuit. Align resonant frequency f_0 with desired frequency δf to give δ. On left-hand side, align δ with Q to give response on Z scale.

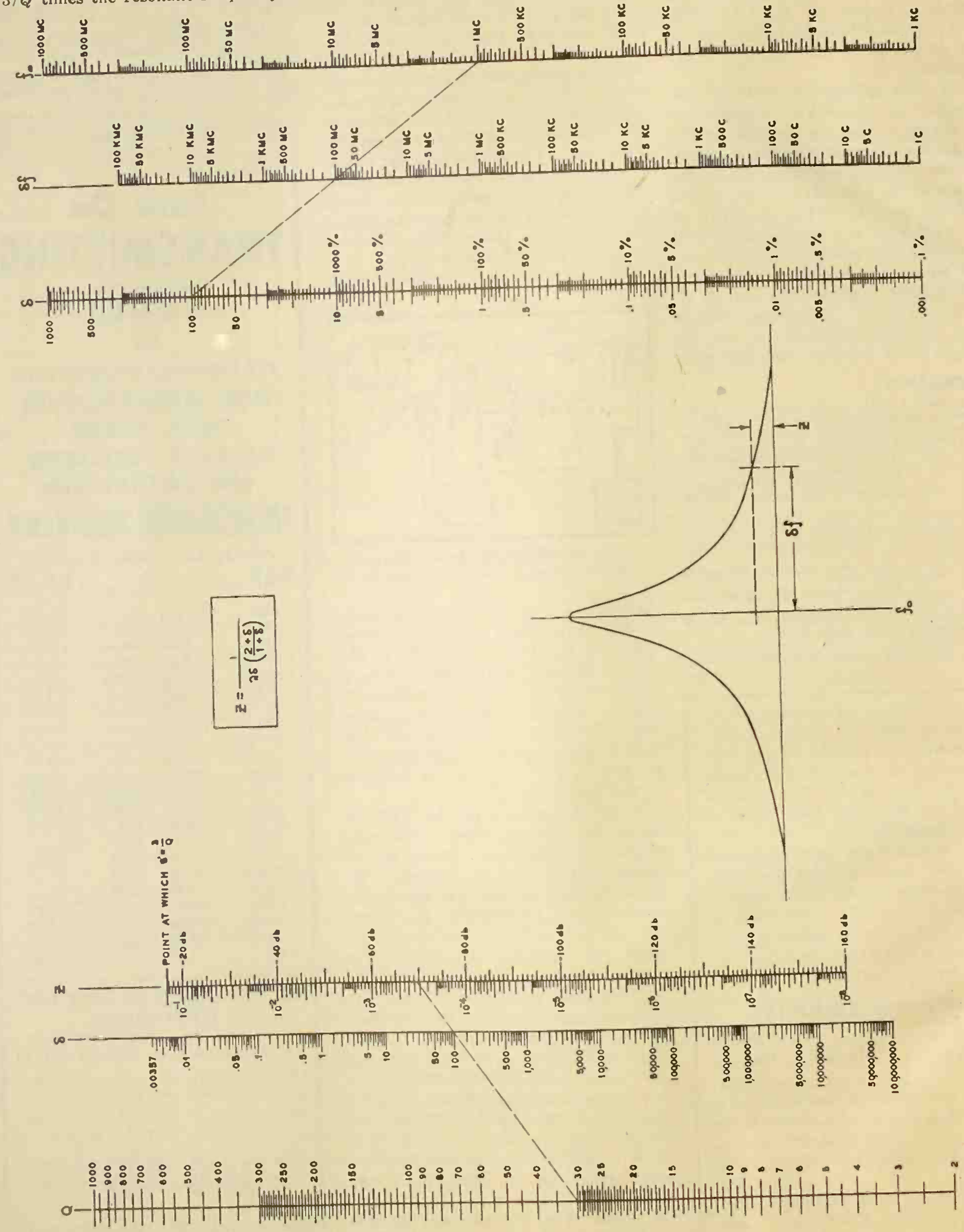

$$Z = \frac{1}{Q\delta\left(\frac{2+\delta}{1+\delta}\right)}$$

Courtesy of Consolidated Vultee Aircraft Corp.


SPRAYBERRY TELEVISION